

УДК 539.12

NUCLEAR SPIN STRUCTURE
IN DARK-MATTER SEARCH:
THE ZERO MOMENTUM TRANSFER LIMIT

V. A. Bednyakov

Joint Institute for Nuclear Research, Dubna

F. Šimkovic

Department of Nuclear Physics, Comenius University, Bratislava, Slovakia

INTRODUCTION	257
THE ZERO MOMENTUM TRANSFER LIMIT	262
SUMMARY AND CONCLUSIONS	282
APPENDIX	283
REFERENCES	288

УДК 539.12

NUCLEAR SPIN STRUCTURE IN DARK-MATTER SEARCH: THE ZERO MOMENTUM TRANSFER LIMIT

V. A. Bednyakov

Joint Institute for Nuclear Research, Dubna

F. Šimkovic

Department of Nuclear Physics, Comenius University, Bratislava, Slovakia

The calculation of spin-dependent matrix elements relevant to scattering of weakly interacting massive particles (WIMP) on nuclei is reviewed. A comprehensive list, to our knowledge, of the proton and neutron total spin expectation values ($\langle S_p \rangle$ and $\langle S_n \rangle$) calculated within different nuclear models is presented. These values allow a conclusion about the event rate expected in direct dark matter search experiments due to spin-dependent neutralino–nucleon interaction, provided neutralino is a dark matter particle.

Дан обзор спиновых ядерных матричных элементов, необходимых для вычисления рассеяния слабо взаимодействующих массивных частиц на ядрах. Приведен наиболее полный список усредненных по ядру значений протонного ($\langle S_p \rangle$) и нейтронного спина ($\langle S_n \rangle$), которые вычислены в рамках ряда ядерных моделей. Эти величины позволяют получить оценки вероятности регистрации частиц темной материи за счет спин-зависимого взаимодействия нейтралино с ядрами в различных экспериментах. При этом предполагается, что нейтралино, будучи легчайшими суперсимметричными частицами, представляют собой частицы темной материи.

INTRODUCTION

Historically, the spin-1/2 weakly interacting massive particles (WIMP) were considered as the first cold dark-matter (DM) candidates. They interact with ordinary matter predominantly by means of axial vector (spin-dependent) and vector (spin-independent) couplings.

Nowadays, the main effort in the direct dark matter search experiments is concentrated on the study of the spin-independent (or scalar) interaction of the dark-matter particles with nuclei. It is due to a strong (proportional to the squared mass of the target nucleus) coherent enhancement of the dark-matter particle scalar interaction with nuclei. The results obtained in the field are presented in the form of the exclusion curves for the total event rate as a function of the mass of the dark-matter particles. The values of the cross section associated with the

elastic scattering of WIMP due to scalar-nucleon interaction, which lie above these curves, are excluded. There is also the so-called DAMA contour which corresponds to the first claim for evidence of the dark-matter signal [1].

The main goal of this review is to attract attention back to the spin-dependent (or axial-vector) interaction of dark-matter particles with nuclei. The importance of this type of interaction of the DM particles is due to the reasons as follows: i) The spin-dependent interaction of the DM particles provides us with twice stronger constraints on the SUSY parameter space in comparison with the spin-independent interaction. ii) In the case of spin-dependent interaction of heavy WIMPs with heavy target nuclei the so-called long q -tail behavior of the relevant form factor allows detection of large nuclear recoil energy due to some nuclear structure effects. iii) It is worthwhile to note that by relying only upon the scalar interaction of the DM particles, which seems to be strongly suppressed, one might miss a DM signal [2]. However, by a simultaneous study of both spin-dependent and spin-independent interactions of the DM particles with nuclei the chance for observing the DM signal is significantly increased.

There are many different nuclear structure calculations (including the case of nonzero momentum transfer) for spin-dependent neutralino interaction with various nuclei, in particular with helium ^3He [3], fluorine ^{19}F [3–5], sodium ^{23}Na [3–6], aluminium ^{27}Al [7], silicon ^{29}Si [4, 5, 8], chlorine ^{35}Cl [8], potassium ^{39}K [7], germanium ^{73}Ge [8, 9], niobium ^{93}Nb [10], iodine ^{127}I [6], xenon ^{129}Xe [6], ^{131}Xe [6, 11, 12], tellurium ^{123}Te [11], tellurium ^{125}Te [6], lead ^{208}Pb [3, 13]. The zero-momentum transfer limits (mostly quenching) were investigated for the target nuclei Cd, Cs, Ba, and La in [11, 14, 15].

A dark matter event is an elastic scattering of a relic neutralino χ (or $\tilde{\chi}$) on the target nucleus (A, Z) , which results in a nuclear recoil with energy E_R detected by a proper detector. The differential event rate in respect to the nuclear recoil energy is a subject of experimental measurements. It depends on the distribution of the relic neutralinos in the solar vicinity $f(v)$ and the cross section of neutralino–nucleus elastic scattering [16–23]. The differential event rate per unit mass of the target material takes the form

$$\frac{dR}{dE_R} = N \frac{\rho_\chi}{m_\chi} \int_{v_{\min}}^{v_{\max}} dv f(v) v \frac{d\sigma}{dq^2}(v, q^2). \quad (1)$$

Here, $N = \mathcal{N}/A$, \mathcal{N} and A stand for the Avogadro number and the atomic mass in AMU, respectively. The typical value of the nuclear recoil energy $E_R = q^2/(2M_A)$ is about $10^{-6}m_\chi$. M_A denotes the nuclear mass.

The neutralino–nucleus elastic scattering cross section for spin-nonzero ($J \neq 0$) nuclei is a sum of the coherent (spin-independent, or SI) and axial (spin-

dependent, or SD) terms [8, 12, 24]:

$$\begin{aligned} \frac{d\sigma^A}{dq^2}(v, q^2) &= \frac{\sum |\mathcal{M}|^2}{\pi v^2(2J+1)} = \frac{S_{\text{SD}}^A(q^2)}{v^2(2J+1)} + \frac{S_{\text{SI}}^A(q^2)}{v^2(2J+1)} = \\ &= \frac{\sigma_{\text{SD}}^A(0)}{4\mu_A^2 v^2} F_{\text{SD}}^2(q^2) + \frac{\sigma_{\text{SI}}^A(0)}{4\mu_A^2 v^2} F_{\text{SI}}^2(q^2). \end{aligned} \quad (2)$$

The normalized-to-unity ($F_{\text{SD,SI}}^2(0) = 1$) nonzero-momentum-transfer nuclear form factors

$$F_{\text{SD,SI}}^2(q^2) = \frac{S_{\text{SD,SI}}^A(q^2)}{S_{\text{SD,SI}}^A(0)} \quad (3)$$

can be expressed through the nuclear structure functions as follows [8, 12, 24]:

$$\begin{aligned} S_{\text{SI}}^A(q) &= \sum_{L \text{ even}} |\langle J || \mathcal{C}_L(q) || J \rangle|^2 \simeq |\langle J || \mathcal{C}_0(q) || J \rangle|^2, \\ S_{\text{SD}}^A(q) &= \sum_{L \text{ odd}} (|\langle N || \mathcal{T}_L^{\text{el5}}(q) || N \rangle|^2 + |\langle N || \mathcal{L}_L^5(q) || N \rangle|^2). \end{aligned} \quad (4)$$

Here, the double vertical lines denote the reduced matrix element. The explicit form of the transverse electric $\mathcal{T}^{\text{el5}}(q)$ and longitudinal $\mathcal{L}^5(q)$ multipole projections of the axial vector current operator, scalar function $\mathcal{C}_L(q)$ and $S_{\text{SI,SD}}^A(q)$ at zero momentum transfer can be found in the Appendix. For $q = 0$ the nuclear SD and SI cross sections (in (2)) take the forms

$$\sigma_{\text{SI}}^A(0) = \frac{4\mu_A^2 S_{\text{SI}}^A(0)}{(2J+1)} = \frac{\mu_A^2}{\mu_p^2} A^2 \sigma_{\text{SI}}^p(0), \quad (5)$$

$$\sigma_{\text{SD}}^A(0) = \frac{4\mu_A^2 S_{\text{SD}}^A(0)}{(2J+1)} = \frac{4\mu_A^2 (J+1)}{\pi J} \{a_p \langle \mathbf{S}_p^A \rangle + a_n \langle \mathbf{S}_n^A \rangle\}^2 = \quad (6)$$

$$= \frac{\mu_A^2 (J+1)}{\mu_{p,n}^2 3J} \left\{ \sqrt{\sigma_{\text{SD}}^p(0)} \langle \mathbf{S}_p^A \rangle + \text{sign}(a_p a_n) \sqrt{\sigma_{\text{SD}}^n(0)} \langle \mathbf{S}_n^A \rangle \right\}^2. \quad (7)$$

Here, $\mu_A = \frac{m_\chi M_A}{m_\chi + M_A}$ is the reduced mass of the neutralino and the nucleus and it is assumed that $\mu_n^2 = \mu_p^2$. The dependence on effective neutralino–quark couplings \mathcal{C}_q and \mathcal{A}_q in the underlying (SUSY) theory (see the Appendix)

$$\mathcal{L}_{\text{eff}} = \sum_q (\mathcal{A}_q \bar{\chi} \gamma_\mu \gamma_5 \chi \bar{q} \gamma^\mu \gamma_5 q + \mathcal{C}_q \bar{\chi} \chi \bar{q} q) + \dots \quad (8)$$

and on the spin ($\Delta_q^{(p,n)}$) and the mass ($f_q^{(p,n)}$) structure of nucleons enter into these formulas via the zero-momentum-transfer proton and neutron SI and SD cross sections:

$$\sigma_{\text{SI}}^p(0) = 4 \frac{\mu_p^2}{\pi} c_0^2, \quad c_0^{p,n} = \sum_q \mathcal{C}_q f_q^{(p,n)}; \quad (9)$$

$$\sigma_{\text{SD}}^{p,n}(0) = 12 \frac{\mu_{p,n}^2}{\pi} a_{p,n}^2, \quad a_p = \sum_q \mathcal{A}_q \Delta_q^{(p)}, \quad a_n = \sum_q \mathcal{A}_q \Delta_q^{(n)}. \quad (10)$$

The factors $\Delta_q^{(p,n)}$, which parameterize the quark spin content of the nucleon, are defined as $2\Delta_q^{(n,p)} s^\mu \equiv \langle p, s | \bar{\psi}_q \gamma^\mu \gamma_5 \psi_q | p, s \rangle_{(p,n)}$. The total nuclear spin (proton, neutron) operator is given by

$$\mathbf{S}_{p,n} = \sum_i^A \mathbf{s}_{p,n}(i), \quad (11)$$

where the index i runs over all nucleons.

The expectation values of the spin and angular operators are evaluated, as a rule, in their z projection by assuming the state with the maximal value of the angular momentum projection $M_J = J$:

$$\langle \mathbf{S} \rangle \equiv \langle N | \mathbf{S} | N \rangle \equiv \langle J, M_J = J | S_z | J, M_J = J \rangle. \quad (12)$$

Thus $\langle \mathbf{S}_{p(n)} \rangle$ is the total spin of protons (neutrons) averaged over all nucleons of the nucleus (A, Z) .

The mean velocity $\langle v \rangle$ of the relic neutralinos of our Galaxy is about $300 \text{ km/s} = 10^{-3}c$. Assuming $q_{\text{max}}R \ll 1$, where R is the nuclear radius and $q_{\text{max}} = 2\mu_A v$ is the maximum of the momentum transfer in the process of the χA scattering, the spin-dependent matrix element takes a simple form (*zero momentum transfer limit*) [6, 7]:

$$\mathcal{M} = C \langle N | a_p \mathbf{S}_p + a_n \mathbf{S}_n | N \rangle \mathbf{s}_\chi = C \Lambda \langle N | \mathbf{J} | N \rangle \mathbf{s}_\chi. \quad (13)$$

Here, \mathbf{s}_χ denotes the spin of the neutralino, and

$$\Lambda = \frac{\langle N | a_p \mathbf{S}_p + a_n \mathbf{S}_n | N \rangle}{\langle N | \mathbf{J} | N \rangle} = \frac{\langle N | (a_p \mathbf{S}_p + a_n \mathbf{S}_n) \mathbf{J} | N \rangle}{J(J+1)}. \quad (14)$$

Note a coupling of the spin of χ to the spin carried by the protons and the neutrons. The uncertainties arising from the electroweak and QCD scale physics are incorporated in the factors a_p and a_n . The normalization factor C involves the coupling constants, the masses of the exchanged bosons and the mixing parameters relevant to the lightest supersymmetric particle (LSP), i.e., it is not related to the

associated nuclear matrix elements [25]. The above conclusions concerning the spin-dependent part of the neutralino–nucleus scattering amplitude are also valid for the amplitude of any Majorana WIMP–nucleus scattering process. In the limit of zero momentum transfer $q = 0$ the spin structure function in Eq. (4) reduces to the form

$$S_{\text{SD}}^A(0) = \frac{2J+1}{\pi} \Lambda^2 J(J+1). \quad (15)$$

The nuclear matrix element \mathcal{M} in Eq. (13) is often related to the matrix element of the nuclear magnetic moment, which also consists of the matrix elements of the total proton and neutron spin operators:

$$\mu = \langle N | g_n^s \mathbf{S}_n + g_n^l \mathbf{L}_n + g_p^s \mathbf{S}_p + g_p^l \mathbf{L}_p | N \rangle. \quad (16)$$

The *free particle* g factors (gyromagnetic ratios) are given (in nuclear magnetons) by:

$$g_n^s = -3.826, \quad g_n^l = 0, \quad g_p^s = 5.586, \quad g_p^l = 1. \quad (17)$$

The nuclear magnetic moment μ is often used as a benchmark for the accuracy of the calculation of \mathbf{S}_p and \mathbf{S}_n [6, 8].

If the neutralino mass m_χ is larger than few tens of GeV, the value of the product qR is no longer negligible and the so-called *finite momentum transfer limit* has to be considered in the case of the neutralino scattering on medium-heavy and heavy nuclei. The corresponding formalism is a generalization of that used for the description of weak and electromagnetic semileptonic interactions in nuclei. We shall follow the conventions of [6, 8]. There is an advantage to use the isospin instead of the proton–neutron representation when discussing χA scattering at finite momentum transfer. By rewriting the isoscalar and isovector coupling constants as $a_0 = a_n + a_p$ and $a_1 = a_p - a_n$, respectively, the spin-dependent cross section $S_{\text{SD}}^A(q)$ decouples into the isoscalar term S_{00} , the isovector term S_{11} , and the interference term S_{01} as follows:

$$S_{\text{SD}}^A(q) = a_0^2 S_{00}(q) + a_1^2 S_{11}(q) + a_0 a_1 S_{01}(q). \quad (18)$$

The structure functions in Eq. (18) consist of the expectation values of operators $j_L(qr)[Y_L \sigma]^{L\pm 1}$ (L even), which depend on spin and spatial coordinates. Using the decomposition of $S_{\text{SD}}^A(q)$ in (18) one can obtain structure functions for χ of arbitrary composition.

The cross section of neutralino–nucleus scattering at zero momentum transfer exhibits a strong dependence on the details of the nuclear ground state [5]. The goal of this review is to collect the results of different calculations and discuss their spread and relevance.

1. THE ZERO MOMENTUM TRANSFER LIMIT

Only nuclei with odd number of either protons or neutrons possess nonzero total nuclear spin. At first, the independent single-particle shell model (ISPSM) was employed by Goodman and Witten [26] and later by others [18, 27, 28] to estimate the spin content of the nucleus for the detection of dark matter. This model utilizes the shell structure of the nucleus, in particular the fact that if certain magic numbers of nucleons occur in the nucleus, it exhibits remarkable stability properties, and the ground state expectation values of the total spin J and the parity of the nucleus can be described by those of the extra nucleon.

For nuclei whose angular momentum J is given by a single neutron (proton) with spin s and the orbital momentum L , $\mathbf{J} = \mathbf{L} + \mathbf{s}$ (the even number of nucleons which remain from pairs with the opposite angular momentum projection and zero spin, i.e., they do not contribute to \mathbf{J}), we have [28]:

$$\langle \mathbf{S}_{n(p)}^A \rangle = \frac{J(J+1) - L(L+1) + 3/4}{2J+2}, \quad \langle \mathbf{S}_{p(n)}^A \rangle = 0. \quad (19)$$

In the ISPSM the entire angular momentum J and the parity of the odd-odd nucleus (A , Z) are identified with a single proton (Z -odd) or neutron (Z -even) state. Then the spin matrix elements are given by Eq. (19).

The ISPSM offers only a rough estimate of the spin matrix elements. From Tables 1–13 it follows that the ISPSM predictions significantly overestimate the values obtained in realistic calculations. The ISPSM results are qualitatively good only for light nuclei with the single nucleon outside the closed shell (e.g., ^{17}O); however, they become increasingly poor for heavier isotopes, especially for those with many particles outside the closed shells. The realistic calculations take into account the complex structure of the nuclear wave functions, the fact that the contributions to spin matrix elements both from paired nucleons and unpaired ones cannot be neglected and the phenomenon that the free nucleon structure coefficients are renormalized when nuclear medium effects are relevant. These effects are known to play an important role in the calculation of the matrix elements of the magnetic dipole moment, too (see, for example, [15]).

There are several elaborated nuclear structure approaches which lead to more accurate predictions of spin matrix elements associated with the dark matter detection on nuclei in comparison with the ISPSM. A full list of these models, to our knowledge, includes the Odd Group Model (OGM) [29] and the extended OGM (EOGM) [24, 29] of Engel and Vogel, the Interacting Boson Fermion Model (IBFM) of Iachello, Krauss, and Maino [15], the theory of Finite Fermi Systems (TFFS) of Nikolaev and Klapdor-Kleingrothaus [30], the Quasi Tamm–Dancoff Approximation (QTDA) of Engel [12], the nuclear shell model (SM) applied by Pacheco and Strottman [14], Engel, Pittel, Ormand and Vogel [10], Engel, Ressel, Towner and Ormand [7], Ressel et al. [8], Ressel and Dean [6];

Table 1. Zero momentum spin structure of light nuclei ($A < 13$) in different models

${}^1\text{H}$ ($L_J = S_{1/2}$)	$\langle \mathbf{S}_p \rangle$	$\langle \mathbf{S}_n \rangle$	μ (in μ_N)
ISPSM, Ellis–Flores [28, 39]	1/2	0	2.793
OGM, Ellis–Flores [28, 39]	0.5	0	$(2.793)_{\text{exp}}$
${}^3\text{He}$ ($L_J = S_{1/2}$)	$\langle \mathbf{S}_p \rangle$	$\langle \mathbf{S}_n \rangle$	μ (in μ_N)
ISPSM, Ellis–Flores [28, 39]	0	1/2	-1.913
OGM, Engel–Vogel [29]	0	0.56	$(-2.128)_{\text{exp}}$
EOGM ($g_A/g_V = 1$), Engel–Vogel [29]	-0.081	0.552	$(-2.128)_{\text{exp}}$
EOGM ($g_A/g_V = 1.25$), Engel–Vogel [29]	-0.021	0.462	$(-2.128)_{\text{exp}}$
${}^7\text{Li}$ ($L_J = P_{3/2}$)	$\langle \mathbf{S}_p \rangle$	$\langle \mathbf{S}_n \rangle$	μ (in μ_N)
ISPSM, Ellis–Flores [28, 39]	1/2	0	3.793
OGM, Engel–Vogel [29]	0.38	0	$(3.256)_{\text{exp}}$
SM, Pacheco–Strottman [14]	0.497	0.004	—
${}^9\text{Be}$ ($L_J = P_{3/2}$)	$\langle \mathbf{S}_p \rangle$	$\langle \mathbf{S}_n \rangle$	μ (in μ_N)
ISPSM, Ellis–Flores [28, 39]	0	1/2	-1.913
OGM, Engel–Vogel [29]	0	0.31	$(-1.178)_{\text{exp}}$
SM, Pacheco–Strottman [14]	0.007	0.415	—
${}^{11}\text{B}$ ($L_J = P_{3/2}$)	$\langle \mathbf{S}_p \rangle$	$\langle \mathbf{S}_n \rangle$	μ (in μ_N)
ISPSM, Ellis–Flores [28, 39]	1/2	0	3.793
OGM, Engel–Vogel [29]	0.264	0	$(2.689)_{\text{exp}}$
EOGM ($g_A/g_V = 1$), Engel–Vogel [29]	0.292	0.006	$(2.689)_{\text{exp}}$
EOGM ($g_A/g_V = 1.25$), Engel–Vogel [29]	0.264	0.034	$(2.689)_{\text{exp}}$
SM, Pacheco–Strottman [14]	0.292	0.008	—

Note. The measured magnetic moments used as input are enclosed in parentheses.

and by Kosmas, Vergados et al. [3, 5, 13] to different nuclear systems, the so-called «hybrid» model of Dimitrov, Engel and Pittel [9] and the perturbation theory (PT) based on calculations of Engel et al. [7].

The ISPSM predictions are fairly accurate for near-closed-shell nuclei, but further away they tend to overestimate the spin contribution to the magnetic moment. In an open-shell nucleus, the last odd particle polarizes the other nucleons in the direction opposite to its own spin, which results in a spin-quenching effect entirely absent in the single-particle picture. Denying the idea about importance of only the last odd nucleon Engel and Vogel arrived at the «odd-group» model [29] by assuming that the nuclear spin is carried by the «odd» unpaired group of protons or neutrons and only one of either $\langle \mathbf{S}_n^A \rangle$ or $\langle \mathbf{S}_p^A \rangle$ is nonzero. The odd-group spin matrix elements are expressed with the measured nuclear magnetic

Table 2. Zero momentum spin structure of light nuclei ($11 < A < 21$) in different models

$^{13}\text{C} (L_J = P_{1/2})$	$\langle \mathbf{S}_p \rangle$	$\langle \mathbf{S}_n \rangle$	μ (in μ_N)
ISPSM	0	-0.167	0.638
OGM	0	-0.183	$(0.702)_{\text{exp}}$
EOGM ($g_A/g_V = 1$), Engel-Vogel [29]	-0.009	-0.172	$(0.702)_{\text{exp}}$
EOGM ($g_A/g_V = 1.25$), Engel-Vogel [29]	-0.026	-0.155	$(0.702)_{\text{exp}}$
$^{15}\text{N} (L_J = P_{1/2})$	$\langle \mathbf{S}_p \rangle$	$\langle \mathbf{S}_n \rangle$	μ (in μ_N)
ISPSM, Engel-Vogel [29]	-0.167	0	-0.264
OGM, Engel-Vogel [29]	-0.167	0	$(-0.283)_{\text{exp}}$
EOGM ($g_A/g_V = 1$), Engel-Vogel [29]	-0.145	0.037	$(-0.283)_{\text{exp}}$
EOGM ($g_A/g_V = 1.25$), Engel-Vogel [29]	-0.127	0.019	$(-0.283)_{\text{exp}}$
$^{17}\text{O} (L_J = D_{5/2})$	$\langle \mathbf{S}_p \rangle$	$\langle \mathbf{S}_n \rangle$	μ (in μ_N)
ISPSM, Ellis-Flores [28, 39]	0	1/2	-1.913
OGM, Engel-Vogel [29]	0	0.49	$(-1.894)_{\text{exp}}$
EOGM ($g_A/g_V = 1$), Engel-Vogel [29]	-0.036	0.508	$(-1.894)_{\text{exp}}$
EOGM ($g_A/g_V = 1.25$), Engel-Vogel [29]	0.019	0.453	$(-1.894)_{\text{exp}}$
SM, Pacheco-Strottman [14]	0	0.5	—
$^{19}\text{F} (L_J = S_{1/2})$	$\langle \mathbf{S}_p \rangle$	$\langle \mathbf{S}_n \rangle$	μ (in μ_N)
ISPSM, Ellis-Flores [28, 39]	1/2	0	2.793
OGM, Engel-Vogel [29]	0.46	0	$(2.629)_{\text{exp}}$
EOGM ($g_A/g_V = 1$), Engel-Vogel [29]	0.415	-0.047	$(2.629)_{\text{exp}}$
EOGM ($g_A/g_V = 1.25$), Engel-Vogel [29]	0.368	-0.001	$(2.629)_{\text{exp}}$
SM, Pacheco-Strottman [14]	0.441	-0.109	—
SM, Divari et al. [5]	0.4751	-0.0087	2.91

moment μ as

$$\langle \mathbf{S}_p^A \rangle = \frac{\mu - g_p^l J}{g_p^s - g_p^l} = \frac{\mu - J}{4.586}, \quad \langle \mathbf{S}_n^A \rangle = \frac{\mu - g_n^l J}{g_n^s - g_n^l} = \frac{-\mu}{3.826}, \quad (20)$$

where g denote gyromagnetic factors of the free nucleon (see (17)). The OGM has been found successful, e.g., in the case of ^{29}Si with $J = 1/2$ and unpaired neutrons. The experimental value of the nuclear magnetic moment $\mu = -0.555$ implies $\langle \mathbf{S}_p^{29} \rangle \approx 0$, and $\langle \mathbf{S}_n^{29} \rangle \approx 0.15$, which is [16] in good agreement with the shell-model calculation of Ressel et al. [8]. The results of OGM calculations are collected in Tables 1–13. We note that for ^{73}Ge with a complex nuclear structure the odd-group model prediction disagrees with the realistic calculation of [8, 9].

The odd-group model is a significant improvement in comparison with the ISPSM. The weak points of this approach are the facts that the roles of small but

Table 3. Zero momentum spin structure of light nuclei ($19 < A < 29$) in different models

$^{21}\text{Ne} (L_J = P_{3/2})$	$\langle \mathbf{S}_p \rangle$	$\langle \mathbf{S}_n \rangle$	μ (in μ_N)
ISPSM	0	1/2	-1.913
OGM	0	0.173	$(-0.662)_{\text{exp}}$
EOGM ($g_A/g_V = 1$), Engel-Vogel [29]	0.020	0.294	$(-0.662)_{\text{exp}}$
EOGM ($g_A/g_V = 1.25$), Engel-Vogel [29]	0.047	0.2646	$(-0.662)_{\text{exp}}$
$^{23}\text{Na} (L_J = P_{3/2})$	$\langle \mathbf{S}_p \rangle$	$\langle \mathbf{S}_n \rangle$	μ (in μ_N)
ISPSM	1/2	0	3.793
SM, Ressel-Dean [6]	0.2477	0.0198	2.2196
OGM, Ressel-Dean [6]	0.1566	0.0	$(2.218)_{\text{exp}}$
SM, Divari et al. [5]	0.2477	0.0199	2.22
$^{25}\text{Mg} (L_J = D_{5/2})$	$\langle \mathbf{S}_p \rangle$	$\langle \mathbf{S}_n \rangle$	μ (in μ_N)
ISPSM	0	1/2	-1.913
OGM	0	0.223	$(-0.855)_{\text{exp}}$
EOGM ($g_A/g_V = 1$), Engel-Vogel [29]	0.040	0.376	$(-0.855)_{\text{exp}}$
EOGM ($g_A/g_V = 1.25$), Engel-Vogel [29]	0.073	0.343	$(-0.855)_{\text{exp}}$
$^{27}\text{Al} (L_J = D_{5/2})$	$\langle \mathbf{S}_p \rangle$	$\langle \mathbf{S}_n \rangle$	μ (in μ_N)
ISPSM, Ellis-Flores [28, 39]	1/2	0	4.793
OGM, Engel-Vogel [29]	0.25	0	$(3.642)_{\text{exp}}$
EOGM ($g_A/g_V = 1$), Engel-Vogel [29]	0.333	0.043	$(3.642)_{\text{exp}}$
EOGM ($g_A/g_V = 1.25$), Engel-Vogel [29]	0.304	0.072	$(3.642)_{\text{exp}}$
SM, Engel et al. [7]	0.3430	0.0296	3.584

not vanishing angular momenta of the even system and of the meson-exchange currents, which can renormalize the g factors in Eq. (20), are ignored. Engel and Vogel improved the OGM [29] by using additional information about β -decay ft values and measured magnetic momenta of «mirror pairs» for nuclear systems with ($A < 50$). For these nuclei they proposed to use two relations [29]:

$$\left(\frac{g_A}{g_V}\right)^2 (\langle \mathbf{S}_{\text{odd}} \rangle - \langle \mathbf{S}_{\text{even}} \rangle)^2 = \left(\frac{6170}{ft} - 1\right) \frac{J}{J+1}, \quad (21)$$

$$\mu_{\text{IS}} = J + 0.76 (\langle \mathbf{S}_{\text{odd}} \rangle + \langle \mathbf{S}_{\text{even}} \rangle) + \mu_x.$$

Here, g_A and g_V are the axial vector and vector coupling constants, respectively; μ_x is a small correction induced by heavy meson exchange and μ_{IS} is a sum of two mirror magnetic moments (isoscalar moment). For free nucleons we have $g_A = 1.25$ and $g_V = 1.0$. However, in the nuclear matter due to the effect of renormalization the value $g_A/g_V = 1.00 \pm 0.02$ is often considered. For light

Table 4. Zero momentum spin structure of light nuclei ($29 < A < 41$) in different models

$^{29}\text{Si} (L_J = S_{1/2})$	$\langle \mathbf{S}_p \rangle$	$\langle \mathbf{S}_n \rangle$	μ (in μ_N)
ISPSM, Ellis–Flores [28, 39]	0	1/2	-1.913
OGM, Engel–Vogel [29]	0	0.15	$(-0.555)_{\text{exp}}$
EOGM ($g_A/g_V = 1$), Engel–Vogel [29]	0.054	0.204	$(-0.555)_{\text{exp}}$
EOGM ($g_A/g_V = 1.25$), Engel–Vogel [29]	0.069	0.189	$(-0.555)_{\text{exp}}$
SM, Ressel et al. [8]	-0.002	0.13	-0.50
SM, Divari et al. [5]	-0.0019	0.1334	-0.50
$^{31}\text{P} (L_J = S_{1/2})$	$\langle \mathbf{S}_p \rangle$	$\langle \mathbf{S}_n \rangle$	μ (in μ_N)
ISPSM	0.5	0	2.793
OGM	0.138	0	$(1.132)_{\text{exp}}$
EOGM ($g_A/g_V = 1$), Engel–Vogel [29]	0.181	0.032	$(1.132)_{\text{exp}}$
EOGM ($g_A/g_V = 1.25$), Engel–Vogel [29]	0.166	0.047	$(1.132)_{\text{exp}}$
$^{35}\text{Cl} (L_J = D_{3/2})$	$\langle \mathbf{S}_p \rangle$	$\langle \mathbf{S}_n \rangle$	μ (in μ_N)
ISPSM, Ellis–Flores [28, 39]	-0.3	0	0.13
OGM, Engel–Vogel [29]	-0.15	0	$(0.822)_{\text{exp}}$
EOGM, Engel–Vogel [29]	-0.094	0.014	$(0.822)_{\text{exp}}$
SM, Pacheco–Strottman [14]	-0.059	-0.011	—
SM, Ressel et al. [8]	-0.051	-0.0088	—
$^{39}\text{K} (L_J = D_{3/2})$	$\langle \mathbf{S}_p \rangle$	$\langle \mathbf{S}_n \rangle$	μ (in μ_N)
ISPSM	-0.3	0	0.324
OGM	-0.242	0	$(0.391)_{\text{exp}}$
EOGM ($g_A/g_V = 1.0$), Engel–Vogel [29]	-0.196	0.055	$(0.391)_{\text{exp}}$
EOGM ($g_A/g_V = 1.25$), Engel–Vogel [29]	-0.171	0.030	$(0.391)_{\text{exp}}$
PT with Force I, Engel et al. [7]	-0.197	0.051	0.420
PT with Force II, Engel et al. [7]	-0.184	0.054	0.181

nuclei the spin matrix elements $\langle \mathbf{S}_p^A \rangle$ and $\langle \mathbf{S}_n^A \rangle$ evaluated within the extended odd group model (EOGM) [29] are listed in Tables 1–4. We see that there is quite good agreement between the EOGM (with $g_A/g_V = 1.00$) and the more sophisticated shell-model calculations for light odd–even isotopes performed by Pacheco and Strottman [14]. Their calculations for $A < 16$ nuclei assumed the Cohen–Kurath interaction [31] and a complete basis within the p -shell model space. For $A > 16$ the Reid interaction was considered and the basis consisted of all allowed states within the $1s-0d$ shell-model space. The results of [14] are given in Tables 1–4. For heavier mirror nuclei with A close to 50, the shell-model calculations are difficult due to a large amount of configurations which have to be taken into account.

Table 5. Zero momentum spin structure of light nuclei ($45 < A < 73$) in different models

^{47}Ti ($L_J = F_{5/2}$)	$\langle \mathbf{S}_p \rangle$	$\langle \mathbf{S}_n \rangle$	μ (in μ_N)
ISPSM, Ellis–Flores [28, 39]	0	-0.357	1.367
OGM, Engel–Vogel [29]	0	0.21	$(-0.788)_{\text{exp}}$
^{49}Ti ($L_J = F_{7/2}$)	$\langle \mathbf{S}_p \rangle$	$\langle \mathbf{S}_n \rangle$	μ (in μ_N)
ISPSM, Ellis–Flores [28, 39]	0	1/2	-1.913
OGM, Engel–Vogel [29]	0	0.29	$(-1.104)_{\text{exp}}$
^{51}V ($L_J = F_{7/2}$)	$\langle \mathbf{S}_p \rangle$	$\langle \mathbf{S}_n \rangle$	μ (in μ_N)
ISPSM, Ellis–Flores [28, 39]	1/2	0	5.79
OGM, Engel–Vogel [29]	0.36	0	$(5.149)_{\text{exp}}$
^{55}Mn ($L_J = F_{5/2}$)	$\langle \mathbf{S}_p \rangle$	$\langle \mathbf{S}_n \rangle$	μ (in μ_N)
ISPSM, Ellis–Flores [39, 40]	-0.357	0	5.79
OGM, Ellis–Flores [39, 40]	0.264	0	$(3.453)_{\text{exp}}$
^{59}Co ($L_J = F_{7/2}$)	$\langle \mathbf{S}_p \rangle$	$\langle \mathbf{S}_n \rangle$	μ (in μ_N)
ISPSM, Ellis–Flores [39, 40]	1/2	0	5.79
OGM, Ellis–Flores [39, 40]	0.25	0	$(4.627)_{\text{exp}}$
^{67}Zn ($L_J = F_{5/2}$)	$\langle \mathbf{S}_p \rangle$	$\langle \mathbf{S}_n \rangle$	μ (in μ_N)
ISPSM, Ellis–Flores [28, 39]	0	-0.357	1.367
OGM, Engel–Vogel [29]	0	-0.23	$(0.875)_{\text{exp}}$
^{69}Ga ($L_J = P_{3/2}$)	$\langle \mathbf{S}_p \rangle$	$\langle \mathbf{S}_n \rangle$	μ (in μ_N)
ISPSM, Ellis–Flores [28, 39]	0.5	0	3.793
OGM, Engel–Vogel [29]	0.11	0	$(2.017)_{\text{exp}}$
^{71}Ga ($L_J = P_{3/2}$)	$\langle \mathbf{S}_p \rangle$	$\langle \mathbf{S}_n \rangle$	μ (in μ_N)
ISPSM, Ellis–Flores [28, 39]	0.5	0	3.793
OGM, Engel–Vogel [29]	0.23	0	$(2.562)_{\text{exp}}$

The light nucleus ^{27}Al is one of the active ingredients of a very high-resolution and low-threshold sapphire-crystal (Al_2O_3)-based detector for dark matter search. Engel, Ressel, Towner, and Ormand [7] performed calculation of proton and neutron spin expectation values for this isotope with the help of the Lanczos m -scheme shell-model code CRUNCHER [32]. The nucleus ^{27}Al lies in the middle of the sd shell and the m -scheme basis for ^{27}Al contains 80115 Slater determinants. Good agreement between the calculated and measured spectroscopy of excited states was achieved for this nucleus. In addition, the experimental value of the magnetic moment $\mu_{\text{exp}} = 3.6415\mu_N$ ($\mu_N = e\hbar/2m_p$) is

Table 6. Zero momentum spin structure of light nuclei ($71 < A < 95$) in different models

$^{73}\text{Ge} (L_J = G_{9/2})$	$\langle \mathbf{S}_p \rangle$	$\langle \mathbf{S}_n \rangle$	μ (in μ_N)
ISPSM, Ellis–Flores [28, 39]	0	0.5	-1.913
OGM, Engel–Vogel [29]	0	0.23	$(-0.879)_{\text{exp}}$
IBFM, Iachello et al. [8, 15]	-0.009	0.469	-1.785
IBFM (quenched), Iachello et al. [8, 15]	-0.005	0.245	$(-0.879)_{\text{exp}}$
TFFS, Nikolaev–Klapdor-Kleingrothaus [30]	0	0.34	—
SM (small), Ressel et al. [8]	0.005	0.496	-1.468
SM (large), Ressel et al. [8]	0.011	0.468	-1.239
SM (large, quenched), Ressel et al. [8]	0.009	0.372	$(-0.879)_{\text{exp}}$
«Hybrid» SM, Dimitrov et al. [9]	0.030	0.378	-0.920
$^{75}\text{As} (L_J = P_{3/2})$	$\langle \mathbf{S}_p \rangle$	$\langle \mathbf{S}_n \rangle$	μ (in μ_N)
ISPSM, Ellis–Flores [28, 39]	0.5	0	3.793
OGM, Engel–Vogel [29]	-0.01	0	$(1.439)_{\text{exp}}$
$^{79}\text{Br} (L_J = P_{3/2})$	$\langle \mathbf{S}_p \rangle$	$\langle \mathbf{S}_n \rangle$	μ (in μ_N)
ISPSM, Ellis–Flores [28, 39]	0.5	0	3.793
OGM, Engel–Vogel [29]	0.13	0	$(2.106)_{\text{exp}}$
$^{81}\text{Br} (L_J = P_{3/2})$	$\langle \mathbf{S}_p \rangle$	$\langle \mathbf{S}_n \rangle$	μ (in μ_N)
ISPSM, Ellis–Flores [28, 39]	0.5	0	3.793
OGM, Engel–Vogel [29]	0.17	0	$(2.271)_{\text{exp}}$
$^{91}\text{Zr} (L_J = D_{5/2})$	$\langle \mathbf{S}_p \rangle$	$\langle \mathbf{S}_n \rangle$	μ (in μ_N)
ISPSM, Ellis–Flores [28, 39]	0	0.5	-1.913
OGM, Engel–Vogel [29]	0	0.34	$(-1.304)_{\text{exp}}$
$^{93}\text{Nb} (L_J = G_{9/2})$	$\langle \mathbf{S}_p \rangle$	$\langle \mathbf{S}_n \rangle$	μ (in μ_N)
ISPSM, Ellis–Flores [28, 39]	0.5	0	6.793
OGM, Engel–Vogel [29]	0.36	0	$(6.171)_{\text{exp}}$
SM (large), Engel et al. [10]	0.48	0.04	6.36
SM (small), Engel et al. [10]	0.46	0.08	5.88

the nuclear magneton) was reproduced in calculation well. The theoretical value $\mu = 3.584\mu_N$ was obtained with the help of the free-particle g factors [7]. We recall that calculation of the magnetic moment requires evaluation of the same spin matrix elements needed to determine the WIMP structure functions at $q^2 = 0$. The corresponding values of $\langle \mathbf{S}_p^{27} \rangle$ and $\langle \mathbf{S}_n^{27} \rangle$ are given in Table 3. We note that the authors calculated structure functions $S(q)$ of ^{27}Al at $q \neq 0$ as well [7].

In the case of ^{39}K the shell-model diagonalization needed for the calculation of the nuclear spin matrix elements requires severe truncations to the active model

Table 7. Zero momentum spin structure of light nuclei ($95 < A < 115$) in different models

^{99}Ru ($L_J = D_{5/2}$)	$\langle \mathbf{S}_p \rangle$	$\langle \mathbf{S}_n \rangle$	μ (in μ_N)
ISPSM, Ellis–Flores [39,40]	0	1/2	-1.913
OGM, Ellis–Flores [39,40]	0	0.17	$(-0.6381)_{\text{exp}}$
^{101}Ru ($L_J = D_{5/2}$)	$\langle \mathbf{S}_p \rangle$	$\langle \mathbf{S}_n \rangle$	μ (in μ_N)
ISPSM, Ellis–Flores [39,40]	0	1/2	-1.913
OGM, Ellis–Flores [39,40]	0	0.19	$(-0.719)_{\text{exp}}$
^{107}Ag ($L_J = P_{1/2}$)	$\langle \mathbf{S}_p \rangle$	$\langle \mathbf{S}_n \rangle$	μ (in μ_N)
ISPSM, Ellis–Flores [28,39]	-0.167	0	-0.264[-0.07]
OGM, Engel–Vogel [29]	-0.13	0	$(-0.114)_{\text{exp}}$
^{109}Ag ($L_J = P_{1/2}$)	$\langle \mathbf{S}_p \rangle$	$\langle \mathbf{S}_n \rangle$	μ (in μ_N)
ISPSM, Ellis–Flores [28,39]	-0.167	0	-0.264[-0.07]
OGM, Ellis–Flores [39,40]	-0.14	0	$(-0.131)_{\text{exp}}$
^{111}Cd ($L_J = S_{1/2}$)	$\langle \mathbf{S}_p \rangle$	$\langle \mathbf{S}_n \rangle$	μ (in μ_N)
ISPSM, Ellis–Flores [28,39]	0	1/2	-1.913
OGM, Engel–Vogel [29]	0	0.16	$(-0.595)_{\text{exp}}$
^{113}Cd ($L_J = S_{1/2}$)	$\langle \mathbf{S}_p \rangle$	$\langle \mathbf{S}_n \rangle$	μ (in μ_N)
ISPSM, Ellis–Flores [28,39]	0	1/2	-1.913
OGM, Engel–Vogel [29]	0	0.16	$(-0.622)_{\text{exp}}$
IBFM, Iachello et al. [15]	-0.001	0.488	—
IBFM (quenched), Iachello et al. [15]	-0.0	0.162	—
TFFS, Nikolaev–Klapdor-Kleingrothaus [30]	0	0.175	—
^{115}Cd ($L_J = S_{1/2}$)	$\langle \mathbf{S}_p \rangle$	$\langle \mathbf{S}_n \rangle$	μ (in μ_N)
ISPSM, Nikolaev–Klapdor-Kleingrothaus [30]	0	1/2	—
IBFM, Iachello et al. [15]	-0.001	0.488	—
IBFM (quenched), Iachello et al. [15]	-0.0	0.168	—
TFFS, Nikolaev–Klapdor-Kleingrothaus [30]	0	0.195	—
OGM	0	0.169	$(-0.6388)_{\text{exp}}$

space. The problem is that ^{39}K is so near the boundary between the sd and pf shells and excitations of particles into higher shells can have significant effects that are often not well simulated by effective operators. Thus, for this nucleus Engel, Ressel, Towner, and Ormand [7] used an alternative scheme based on perturbation theory (PT) for the evaluation of spin matrix elements. It was successfully implemented in calculations of several spin-dependent observables in closed-shell-plus (or minus)-one nuclei [33]. The details of the method and

Table 8. Zero momentum spin structure of heavy nuclei ($114 < A < 125$) in different models

$^{115}\text{Sn} (L_J = S_{1/2})$	$\langle \mathbf{S}_p \rangle$	$\langle \mathbf{S}_n \rangle$	μ (in μ_N)
ISPSM, Ellis–Flores [28, 39]	0	1/2	-1.913
OGM, Engel–Vogel [29]	0	0.24	$(-0.919)_{\text{exp}}$
$^{117}\text{Sn} (L_J = S_{1/2})$	$\langle \mathbf{S}_p \rangle$	$\langle \mathbf{S}_n \rangle$	μ (in μ_N)
ISPSM, Ellis–Flores [28, 39]	0	1/2	-1.913
OGM, Engel–Vogel [29]	0	0.126	$(-1.001)_{\text{exp}}$
$^{121}\text{Sb} (L_J = D_{5/2})$	$\langle \mathbf{S}_p \rangle$	$\langle \mathbf{S}_n \rangle$	μ (in μ_N)
ISPSM, Ellis–Flores [28, 39]	0.5	0	4.793
OGM, Ellis–Flores [39, 40]	0.188	0	$(3.363)_{\text{exp}}$
$^{123}\text{Sb} (L_J = G_{7/2})$	$\langle \mathbf{S}_p \rangle$	$\langle \mathbf{S}_n \rangle$	μ (in μ_N)
ISPSM, Ellis–Flores [28, 39]	-0.389	0	1.717
OGM, Ellis–Flores [39, 40]	-0.207	0	$(2.550)_{\text{exp}}$
$^{123}\text{Te} (L_J = S_{1/2})$	$\langle \mathbf{S}_p \rangle$	$\langle \mathbf{S}_n \rangle$	μ (in μ_N)
ISPSM, Ellis–Flores [28, 39]	0	1/2	-1.913
IBFM, Iachello et al. [15]	-0.000	0.491	—
IBFM (quenched), Iachello et al. [15]	-0.000	0.192	—
TFFS, Nikolaev–Klapdor–Kleingrothaus [30]		0.21	—
OGM	0	0.192	$(-0.737)_{\text{exp}}$
$^{125}\text{Te} (L_J = S_{1/2})$	$\langle \mathbf{S}_p \rangle$	$\langle \mathbf{S}_n \rangle$	μ (in μ_N)
ISPSM, Ellis–Flores [28, 39]	0	1/2	-1.913
OGM, Engel–Vogel [29]	0.0	0.23	$(-0.889)_{\text{exp}}$
IBFM, Iachello et al. [15]	-0.0008	0.499	$(-0.889)_{\text{exp}}$
IBFM (quenched), Iachello et al. [15]	-0.0004	0.231	$(-0.889)_{\text{exp}}$
TFFS, Nikolaev–Klapdor–Kleingrothaus [30]		0.22	—
SM (Bonn A), Ressel–Dean [6]	0.001	0.287	-1.015 $\{-0.749\}_{\text{eff}}$
SM (Nijmegen II), Ressel–Dean [6]	-0.0003	0.323	-1.134 $\{-0.824\}_{\text{eff}}$

Note. Calculations of the magnetic moment using effective g factors are given in curly brackets.

the calculations can be found in Ref. 7. The authors considered two different residual interactions. One (denoted as I in Table 4) is related to the one-boson-exchange potential of the Bonn type, but it is limited only to four or five important meson exchanges. The resulting interaction has a weak tensor-force component typical of Bonn potentials. The other (denoted as II in Table 4) is represented by full G -matrix elements of the Paris potential parameterized in terms of sums over Yukawa functions of various ranges and strengths. Interaction II exhibits a

Table 9. Zero momentum spin structure of heavy nuclei ($125 < A < 127$) in different models

$^{125}\text{I} (L_J = D_{5/2})$	$\langle \mathbf{S}_p \rangle$	$\langle \mathbf{S}_n \rangle$	μ (in μ_N)
ISPSM, Engel–Vogel [29]	1/2	0	4.793
IBFM, Iachello et al. [15]	0.460	0.005	
IBFM (quenched), Iachello et al. [15]	0.159	0.002	
TFFS, Nikolaev–Klapdor–Kleingrothaus [30]	0.18		
OGM	0.07	0	$(2.821)_{\text{exp}}$
$^{127}\text{I} (L_J = D_{5/2})$	$\langle \mathbf{S}_p \rangle$	$\langle \mathbf{S}_n \rangle$	μ (in μ_N)
ISPSM, Ellis–Flores [39, 40]	1/2	0	4.793
OGM, Engel–Vogel [29]	0.07	0	$(2.813)_{\text{exp}}$
IBFM, Iachello et al. [15]	0.464	0.010	$(2.813)_{\text{exp}}$
IBFM (quenched), Iachello et al. [15]	0.154	0.003	$(2.813)_{\text{exp}}$
TFFS, Nikolaev–Klapdor–Kleingrothaus [30]	0.15	0	—
SM (Bonn A), Ressel–Dean [6]	0.309	0.075	$2.775 \{2.470\}_{\text{eff}}$
SM (Nijmegen II), Ressel–Dean [6]	0.354	0.064	$3.150 \{2.7930\}_{\text{eff}}$
<i>Note.</i> Calculations of the magnetic moment using effective g factors are given in curly brackets.			

strong tensor force. The quality of the wave functions obtained was judged in terms of magnetic moments and Gamow–Teller matrix elements, including meson-exchange currents, isobar currents, and other relativistic effects. The results were presented for both isoscalar and isovector magnetic moments and their sum, i.e., for the magnetic moment of ^{39}K , whose value is given in Table 4. The magnetic moments calculated with the help of both interactions differ only slightly from each other and showed good agreement with corresponding experimental values. The same nuclear wave functions of ^{39}K were also used for the calculation of $\langle \mathbf{S}_p^{39} \rangle$ and $\langle \mathbf{S}_n^{39} \rangle$ (Table 4) and the structure function $S(q)$ [7]. It is worthwhile to notice that for both types of interactions the zero-momentum transfer spin matrix elements coincide well with those obtained within the phenomenological EOGM [29].

For dark matter targets constructed of heavy nuclei, in particular, Ge, I, and Xe, the first elaborated calculation of spin-dependent matrix elements relevant to WIMP scattering was performed by Iachello, Krauss, and Maino within the Interacting Boson Fermion Model (IBFM) [15]. The applied IBFM wave functions were tested in a comprehensive analysis of excitation energies, electromagnetic transition rates and intensities of transfer reactions [15]. In this model the total spin operator has the form $S = \sum s_p^\pi + \sum s_n^\nu + s_{p,n}$, where $s_{p(n)}^{\pi(\nu)}$ are the paired proton (neutron) spins, and $s_{p(n)}$ is the remaining unpaired proton (neutron) spin. To estimate the matrix elements of the paired nucleons one should know the struc-

Table 10. Zero momentum spin structure of heavy nuclei ($128 < A < 133$) in different models

$^{129}\text{Xe} (L_J = S_{1/2})$	$\langle \mathbf{S}_p \rangle$	$\langle \mathbf{S}_n \rangle$	μ (in μ_N)
ISPSM, Ellis–Flores [28, 39]	0	1/2	−1.913
OGM, Engel–Vogel [29]	0.0	0.2	(−0.778) _{exp}
IBFM, Iachello et al. [15]	−0.000	0.430	(−0.778) _{exp}
IBFM (quenched), Iachello et al. [15]	−0.000	0.200	(−0.788) _{exp}
TFFS, Nikolaev–Klapdor–Kleingrothaus [30]		0.25	—
SM (Bonn A), Ressel–Dean [6]	0.028	0.359	−0.983 {−0.634} _{eff}
SM (Nijmegen II), Ressel–Dean [6]	0.0128	0.300	−0.701 {−0.379} _{eff}
$^{131}\text{Xe} (L_J = D_{3/2})$	$\langle \mathbf{S}_p \rangle$	$\langle \mathbf{S}_n \rangle$	μ (in μ_N)
ISPSM, Ellis–Flores [28, 39]	0	−0.3	1.148
OGM, Engel–Vogel [29]	0.0	−0.18	(0.692) _{exp}
IBFM, Iachello et al. [15]	0.000	−0.280	(0.692) _{exp}
IBFM (quenched), Iachello et al. [15]	0.000	−0.168	(0.692) _{exp}
TFFS, Nikolaev–Klapdor–Kleingrothaus [30]		−0.186	—
SM (Bonn A), Ressel–Dean [6]	−0.009	−0.227	0.980 {0.637} _{eff}
SM (Nijmegen II), Ressel–Dean [6]	−0.012	−0.217	0.979 {0.347} _{eff}
QTDA, Engel [12]	−0.041	−0.236	0.70
$^{133}\text{Xe} (L_J = D_{3/2})$	$\langle \mathbf{S}_p \rangle$	$\langle \mathbf{S}_n \rangle$	μ (in μ_N)
ISPSM, Ellis–Flores [28, 39]	0	−0.3	1.148
IBFM, Iachello et al. [15]	0.000	−0.257	
IBFM (quenched), Iachello et al. [15]	0.000	−0.176	
TFFS, Nikolaev–Klapdor–Kleingrothaus [30]		−0.201	
OGM	0.0	−0.213	(0.813) _{exp}

Note. Calculations of the magnetic moment using effective g factors are given in curly brackets.

ture of Cooper pairs (bosons), which were incorporated in the model by fitting the matrix elements of the magnetic moments. The authors end with the conclusion that the ISPSM predictions are generally within 15% of their results for the nucleon spin matrix elements [15]. If quenching of free-particle coefficients in the nuclear environment is considered, the value of the spin matrix elements is reduced by an additional factor not exceeding 60%. The results obtained are listed in Tables 6–11. We note that the spin-dependent WIMP-nucleus cross section associated with the IBFM spin matrix elements is always smaller than the ISPSM prediction but not more than a factor of 5 [15]. While the IBFM can incorporate the dominant collective effects, it has some difficulty in including the spin polarization, which plays a crucial role in axial vector scattering. Unfortunately, this approach cannot be readily applied to the case of nonzero momentum transfer [5].

Table 11. Zero momentum spin structure of heavy nuclei ($133 < A < 141$) in different models

$^{133}\text{Cs} (L_J = G_{7/2})$	$\langle \mathbf{S}_p \rangle$	$\langle \mathbf{S}_n \rangle$	μ (in μ_N)
ISPSM, Ellis–Flores [28, 39]	−0.389	0	1.717
OGM, Engel–Vogel [29]	−0.20	0	(2.582) _{exp}
IBFM, Iachello et al. [15]	−0.370	0.003	
IBFM (quenched), Iachello et al. [15]	−0.225	0.002	
TFFS, Nikolaev–Klapdor-Kleingrothaus [30]	−0.230		
$^{135}\text{Cs} (L_J = G_{7/2})$	$\langle \mathbf{S}_p \rangle$	$\langle \mathbf{S}_n \rangle$	μ (in μ_N)
ISPSM, Ellis–Flores [28, 39]	−0.389	0	1.717
OGM	−0.167	0	(2.734) _{exp}
IBFM, Iachello et al. [15]	−0.373	0.002	
IBFM (quenched), Iachello et al. [15]	−0.201	0.001	
TFFS, Nikolaev–Klapdor-Kleingrothaus [30]	−0.199		
$^{135}\text{Ba} (L_J = D_{3/2})$	$\langle \mathbf{S}_p \rangle$	$\langle \mathbf{S}_n \rangle$	μ (in μ_N)
ISPSM, Ellis–Flores [28, 39]	0	−0.30	1.148
OGM	0	−0.219	(0.838) _{exp}
IBFM, Iachello et al. [15]	−0.007	−0.226	
IBFM (quenched), Iachello et al. [15]	−0.004	−0.145	
TFFS, Nikolaev–Klapdor-Kleingrothaus [30]		−0.18	
$^{137}\text{La} (L_J = G_{7/2})$	$\langle \mathbf{S}_p \rangle$	$\langle \mathbf{S}_n \rangle$	μ (in μ_N)
ISPSM, Ellis–Flores [28, 39]	−0.389	0	1.717
OGM	−0.176	0	(2.695) _{exp}
IBFM, Iachello et al. [15]	−0.386	0.0006	
IBFM (quenched), Iachello et al. [15]	−0.212	0.0003	
$^{139}\text{La} (L_J = G_{7/2})$	$\langle \mathbf{S}_p \rangle$	$\langle \mathbf{S}_n \rangle$	μ (in μ_N)
ISPSM, Ellis–Flores [28, 39]	−0.389	0	1.717
OGM, Engel–Vogel [29]	−0.16	0	(2.783) _{exp}

In [5], Vergados with coauthors investigated the spin-dependent elastic neutralino scattering with light nuclei ^{19}F , ^{23}Na , and ^{29}Si . The spin contribution to the differential cross section was obtained by the shell-model calculations in the sd shell using the Wildenthal interaction, which was developed and tested over many years. This interaction is known to reproduce accurately many nuclear observables for sd shell nuclei. The Wildenthal two-body matrix elements as well as the single-particle energies are determined by fits to experimental data in nuclei from $A = 17$ to $A = 39$. The shell-model wave functions used by the authors were tested in the calculation of the low-energy spectra and ground

Table 12. Zero momentum spin structure of heavy nuclei ($143 < A < 205$) in different models

$^{155}\text{Gd} (L_J = P_{3/2})$	$\langle \mathbf{S}_p \rangle$	$\langle \mathbf{S}_n \rangle$	μ (in μ_N)
ISPSM, Ellis–Flores [39,40]	0	0.5	-1.913
OGM, Ellis–Flores [39,40]	0	0.07	$(-0.259)_{\text{exp}}$
$^{157}\text{Gd} (L_J = P_{3/2})$	$\langle \mathbf{S}_p \rangle$	$\langle \mathbf{S}_n \rangle$	μ (in μ_N)
ISPSM, Ellis–Flores [39,40]	0	0.5	-1.913
OGM, Ellis–Flores [39,40]	0	0.09	$(-0.340)_{\text{exp}}$
$^{183}\text{W} (L_J = P_{1/2})$	$\langle \mathbf{S}_p \rangle$	$\langle \mathbf{S}_n \rangle$	μ (in μ_N)
ISPSM, Ellis–Flores [39,40]	0	-0.17	0.638
OGM, Ellis–Flores [39,40]	0	-0.03	$(0.118)_{\text{exp}}$
$^{191}\text{Ir} (L_J = D_{3/2})$	$\langle \mathbf{S}_p \rangle$	$\langle \mathbf{S}_n \rangle$	μ (in μ_N)
ISPSM, Ellis–Flores [39,40]	-0.30	0	0.148
OGM, Ellis–Flores [39,40]	-0.295	0	$(0.151)_{\text{exp}}$
$^{193}\text{Ir} (L_J = D_{3/2})$	$\langle \mathbf{S}_p \rangle$	$\langle \mathbf{S}_n \rangle$	μ (in μ_N)
ISPSM, Ellis–Flores [39,40]	-0.30	0	0.148
OGM, Ellis–Flores [39,40]	-0.292	0	$(0.164)_{\text{exp}}$
$^{199}\text{Hg} (L_J = P_{1/2})$	$\langle \mathbf{S}_p \rangle$	$\langle \mathbf{S}_n \rangle$	μ (in μ_N)
ISPSM, Ellis–Flores [28,39]	0	-0.17	0.638
OGM, Engel–Vogel [29]	0	-0.13	$(0.506)_{\text{exp}}$
$^{201}\text{Hg} (L_J = P_{3/2})$	$\langle \mathbf{S}_p \rangle$	$\langle \mathbf{S}_n \rangle$	μ (in μ_N)
ISPSM, Ellis–Flores [39,40]	0	0.5	-1.913
OGM, Ellis–Flores [39,40]	0	0.146	$(-0.560)_{\text{exp}}$
$^{203}\text{Tl} (L_J = S_{1/2})$	$\langle \mathbf{S}_p \rangle$	$\langle \mathbf{S}_n \rangle$	μ (in μ_N)
ISPSM, Ellis–Flores [28,39]	0.50	0	2.793
OGM, Engel–Vogel [29]	0.24	0	$(1.662)_{\text{exp}}$
$^{205}\text{Tl} (L_J = S_{1/2})$	$\langle \mathbf{S}_p \rangle$	$\langle \mathbf{S}_n \rangle$	μ (in μ_N)
ISPSM, Ellis–Flores [28,39]	0.50	0	2.793
OGM, Engel–Vogel [29]	0.25	0	$(1.638)_{\text{exp}}$

state magnetic moment. Rather good agreement between theoretical results and experimental data was achieved. This fact increases the confidence level of the calculated spin matrix elements which are listed in Tables 2–4. It is worth mentioning that these spin matrix elements are in good agreement with those of previous calculations [8]. The authors of Ref. 5 found ^{19}F to be the most favorable target for dark matter search via spin-dependent interaction of relatively light

Table 13. Zero momentum spin structure of heavy nuclei ($A < 209$) in different models

^{207}Pb ($L_J = P_{1/2}$)	$\langle \mathbf{S}_p \rangle$	$\langle \mathbf{S}_n \rangle$	μ (in μ_N)
ISPSM, Ellis–Flores [28, 39]	0	-0.17	0.638
OGM, Engel–Vogel [29]	0	-0.15	$(0.593)_{\text{exp}}$
SM, Kosmas–Vergados [3, 13]	-0.010	-0.149	
^{209}Bi ($L_J = H_{9/2}$)	$\langle \mathbf{S}_p \rangle$	$\langle \mathbf{S}_n \rangle$	μ (in μ_N)
ISPSM, Ellis–Flores [39, 40]	-0.41	0	2.63
OGM, Ellis–Flores [39, 40]	-0.085	0	$(4.111)_{\text{exp}}$

dark matter particles. It is favored due to the fact that the corresponding spin matrix element is not quenched and that various isospin channels add coherently. Further, it was demonstrated that the effect of the nuclear structure on the elastic scattering cross section of LSP with light nuclei (including $q \neq 0$ behavior) is well understood, both for coherent and spin modes [4, 5].

The Theory of Finite Fermi Systems (TFFS) was used by Nikolaev and Klapdor-Kleingrothaus [30] to describe spin matrix elements in the nuclear medium and to evaluate quenching of zero-momentum nuclear spin matrix elements of heavy nuclei due to residual interactions. Contrary to the OGM and the IFBM studies the TFFS calculation of spin matrix elements is not related with the experimental value of the associated magnetic moment. The TFFS proton and neutron spin averages $\langle \mathbf{S}_{p(n)} \rangle$ are suppressed in comparison with the corresponding ISPSM predictions and in some cases they differ significantly from the OGM values, too [29]. However, they agree well (with exception of the case of ^{73}Ge) with the results obtained by Pacheco and Strottman [14] in a completely different IFBM approach (Tables 6–11).

The momentum transfer dependence of the structure function $S(q)$ associated with scattering of dark-matter particles from ^{131}Xe , a promising heavy target for the dark-matter search experiment, was investigated by Engel [12] by using the configuration-mixing quasiparticle Tamm–Dancoff approximation (QTDA). In the zeroth order the ground state of ^{131}Xe was represented as the $1d_{3/2}$ quasi-neutron excitation of the even–even core $|0\rangle$ treated in the BCS approximation (BCS-based model of the Fermi surface). In the case of odd-multipole operators (4) the one-quasiparticle approximation corresponds to the ISPSM approach of [28]. In order to incorporate nuclear structure corrections originating from the residual interaction, three-quasiparticle configurations of the form $[\nu_{d_{3/2}}^\dagger [\nu_k^\dagger \nu_l^\dagger]^K]^{3/2} |0\rangle$ and $[\nu_{d_{3/2}}^\dagger [\pi_k^\dagger \pi_l^\dagger]^K]^{3/2} |0\rangle$ were admixed. Here π^\dagger and ν^\dagger represent the proton and neutron quasiparticle creation operators, K is an arbitrary intermediate angular momentum, and k, l run over a valence space consisting of the $2s, 1d, 0g,$ and $0h$ harmonic oscillator levels [12]. Despite the fact that the

amplitudes associated with the admixed three-quasiparticle states are small (less than 5%), these admixtures can lead to a substantial effect. The experimental value of the magnetic moment of ^{131}Xe , which is about $0.69\mu_N$, was reproduced with an accuracy of 2% in the QTDA (note that the ISPSM value is almost twice larger). The same approximation scheme results in $\langle \mathbf{S}_p^{131} \rangle = -0.041$ and $\langle \mathbf{S}_n^{131} \rangle = -0.236$ (Table 10).

The neutralino–nucleus cross section associated with the spin-dependent interaction is determined by the distribution of the spin in the nucleus. This observable is difficult to describe accurately as the lowest order nucleons create pairs with zero spin. The spin-dependent scattering mostly takes place near the nuclear Fermi surface and it is affected by the behavior of relatively few nucleons. The silicon nucleus is relatively light. Thus, shell-model calculations or arguments based on existing data of magnetic moments (OGM and EOGM) allow a reliable prediction of deviations from the simple ISPSM picture. A different type isotope is germanium with a complex nuclear structure. For this nucleus the reliable calculation of spin expectation values is rather difficult. Niobium isotope ^{93}Nb is something in between the above two special cases. It is a heavy nucleus, which can be represented by a basic shell-model space corresponding to three protons in the $1p_{1/2}$ or $0g_{9/2}$ levels and two neutrons in the $1d_{5/2}$ level [10]. This model space was considered by Engel, Pittel, Ormand, and Vogel [10] in the calculation of the magnetic moment for this isotope. They found μ to be equal to $6.36\mu_N$, which exceeds the experimental value $\mu = 6.17\mu_N$. In order to obtain better agreement with the experiment the authors considered a «large» model space which included all basis states in which one proton or one neutron is excited from the small model space. Then, they ended up with the magnetic moment equal to $5.88\mu_N$, a value that is smaller. The explanation could be that meson-exchange currents renormalize orbital proton g factors upwards by about 10%, increasing the μ without altering the values of the nuclear spin matrix elements. The discrepancy between the $\langle \mathbf{S}_{p,n}^{93} \rangle$ results obtained within the small and large model spaces (Table 6) provides an indication of uncertainty of the nuclear-structure calculation [10].

Germanium isotopes (especially large-spin ^{73}Ge) are considered to be the most promising material for the direct dark matter search experiment. However, there are fundamental difficulties in describing, e.g., the spin content of ^{73}Ge due to its complicated collective structure. Several studies were devoted to nuclear structure aspects of spin-dependent scattering of neutralinos from ^{73}Ge . Engel and Vogel (OGM) [29] used measured magnetic moments to estimate the quenching of the nucleon spin in several heavy nuclei, including germanium. Iachello, Krauss, and Maino [15] employed the IBFM, and Nikolaev and Klapdor-Kleingrothaus [30] used the TFFS to calculate the same quantities. There are two most comprehensive spin structure analyses for ^{73}Ge . A large-basis shell-model study was performed by Ressel et al. [8], who calculated the full spin-dependent

neutralino response including q dependence of form factors. An equally comprehensive calculation was realized by Dimitrov, Engel, and Pittel [9]. The authors obtained significantly different results in comparison with other studies and they argue that their results are more reliable than the previous ones.

By using a reasonable two-body interaction Hamiltonian and appropriate large model spaces, Ressel et al. [8] calculated the ground state wave functions for ^{29}Si and ^{73}Ge . In particular, the universal sd shell interaction of Wildenthal was used for calculation of the wave functions for silicon. The nuclear wave functions obtained were tested in the analysis of energy pattern of excited states and magnetic moments. Once reasonable agreement among theoretical results and experimental data was obtained, the ground-state wave functions were used to calculate the neutralino–nucleus nuclear matrix elements. In addition, finite momentum transfer matrix elements and cross sections for the spin-dependent elastic scattering of neutralinos from ^{29}Si and ^{73}Ge [8] were evaluated. The computations were performed by using the Lanczos method m -scheme nuclear shell model (code CRUNCHER) [32]. The m -scheme basis for ^{29}Si had a dimension of 80115 Slater determinants. In the limit of zero momentum transfer the scattering matrix elements for ^{29}Si are in general agreement with previous estimates (Table 4).

For the study of ^{73}Ge , Ressel et al. [8] chose the Petrovich–McManus–Madsen–Atkinson interaction [34], which is a reasonable approximation to a full G -matrix calculation. This interaction proved to be both adequate and tractable in shell-model applications. Two different model spaces were considered. The «small» space was determined by an m -scheme basis dimension of 24731 Slater determinants. The «large» space allowed much more excitations with an m -scheme basis dimension of 117137 Slater determinants. Despite fairly large size of the bases, rather severe truncations in the space were enacted. The small space is the smallest one in which it is possible to obtain agreement with the experimental spectrum energy levels. The dimension of the large basis was limited by the computer time and the memory storing constraints [8]. No phenomenological interaction has been developed for Ge-like nuclei and fairly severe truncations to the model space have to be imposed to obtain manageable dimensions. Despite these obstacles, the ground state wave function for ^{73}Ge allowed good description of the low-lying excited states and the ground state to ground-state spectroscopic factor. The large model space wave function of ^{73}Ge led to an improved description of the ground state expectation values, in particular of the value of the magnetic moment, in comparison with the ISPSM and IBFM estimates. The calculated magnetic moment μ from [8] exceeds the experiment value, but the authors stressed that the same quenching of both μ and the Gamov–Teller (GT) spin matrix elements was almost universally required in shell-model calculations of all heavy nuclei. Assuming the isovector spin quenching factor to be 0.833, agreement with the measured μ is obtained. In principle, it is not obvious that quenching is really needed in neutralino- ^{71}Ge scattering but if so, Ressel et al.

believed that the correct answer might be in the range between the quenched and unquenched values. It was found (Table 6) that the zero-momentum-transfer spin-neutron matrix element $\langle \mathbf{S}_n^{73} \rangle$ of ^{73}Ge was a factor of 2 larger than the previous predictions (except, obviously, the ISPSM value). Thus, even if quenching is assumed, the calculated scattering rate is about twice as large as any of the estimates made before [8].

A different sophisticated approach for evaluation of the spin structure of ^{73}Ge was considered by Dimitrov, Engel, and Pittel. It relies on the idea of mixing variationally determined Slater determinants, in which symmetries are broken but restored either before or after variation. This approach is described in detail in [35]. In the calculation of [9] the symmetries broken in the intrinsic states are those associated with rotational invariance, parity, and axial shape. The hybrid procedure used restores axial symmetry, parity invariance, and approximate rotational invariance prior to the variation of each intrinsic state. Subsequently, before mixing the intrinsic states the rotational invariance is fully restored. The procedure allows fully triaxial Slater determinants at the expense of particle-number breaking. The results of [35] indicate that the trading of number nonconservation for triaxiality is a good idea, despite the apparent loss of pairing correlations traditionally associated with the former. Pairing forces evidently induce effective triaxiality. The numerical results [35] show that the approach is accurate and efficient for describing even–even systems while also providing reliable reproduction of the collective dynamics of odd-mass systems [9].

For ^{73}Ge the calculations were performed by assuming, both for protons and neutrons, a single-particle model consisting of the full $0f, 1p$ shell and the $0g_{9/2}$ and $0g_{7/2}$ levels. The main idea was to include all the single-particle orbits that could play an important role in reproducing low-energy properties of the ^{73}Ge [9]. It is well known that a crucial ingredient in any realistic nuclear-structure calculation is the appropriate form of the nuclear Hamiltonian. The one- and two-body parts of the Hamiltonian have to be compatible with each other as well as with the model space. This is difficult to achieve because microscopic two-body interactions, derived for example from a G -matrix, include monopole pieces that are unable to describe the movement of spherical single-particle levels as one passes from the beginning to the end of a shell. A proposed procedure for avoiding this problem consists basically in removing all monopole components from the two-body interaction and shifting their effects to the single-particle energies. This procedure was used by Dimitrov, Engel, and Pittel [9] — their two-body force was a fit to Paris-potential G matrix modified as just described above. The calculated ground-state magnetic dipole moment is in good agreement with the experimental value. Ressel et al. [8] in their large space shell-model calculation were able to reduce μ significantly to $-1.24\mu_N$ (without direct quenching) but could not account for the remaining difference. On the contrary, the calculation of Dimitrov, Engel, and Pittel, despite the small number of intrinsic states, contains

the full quenching required by experiment [9]. By making a comparison with the results of Ressel et al. again [8], significant disagreement is found for the neutron spin. The calculated value of Dimitrov, Engel, and Pittel is significantly smaller (Table 6). The large and negative neutron spin g factor ($g_n^s = -3.826$) is favored by the correct μ value. The differences in the spins, unlike those in the orbital angular momenta, carry over into WIMP scattering cross sections. Thus, following Ressel et al. [8], no significant increase is expected in the neutralino- ^{73}Ge scattering rate.

The advantage of Dimitrov, Engel, and Pittel's approach for calculation of neutralino cross sections is that it correctly represents the spin structure, requires neither quenching at $q = 0$ nor arbitrary assumptions about the form factor behavior at $q \neq 0$ [9]. The spin matrix elements depend in general rather sensitively on the details of the nuclear structure. Since the matrix elements at $q = 0$ are often quenched, the momentum dependence of the matrix elements was more important than it was naively expected. As a matter of fact, one has to include a lot of configurations to accommodate all multipoles, which result in very large Hilbert spaces in complex nuclei like ^{29}Si and ^{73}Ge . It will be therefore a very hard task to substantially improve the calculations of Ressel et al. [8] and Dimitrov, Engel, and Pittel [9] for these elements.

For evaluations of the spin matrix elements in the heaviest possible nuclei relevant to dark matter search, Kosmas, and Vergados have chosen ^{207}Pb [3, 13]. Among the targets which were considered for direct neutralino detection, ^{207}Pb stands out as an important candidate. The spin matrix element of this nucleus has not been evaluated quite accurately, since one expected that the neutralino spin interaction is important only with light nuclei. But the spin matrix element in the light systems is quenched. On the other hand, the spin matrix element of ^{207}Pb , especially the isoscalar one, does not suffer unusually large quenching, as is known from the study of the magnetic moment. It is believed that ^{207}Pb has a quite simple structure, its ground state can be described as a $2p_{1/2}$ neutron hole outside the doubly magic (closed-shell) nucleus ^{208}Pb . Due to its low angular momentum, only two multipoles $L = 0$ and $L = 2$ can contribute even at large momentum transfers. One can thus view the information obtained from this simple nucleus as complementary to that of ^{73}Ge , which has a very complex nuclear structure [3, 13]. In the $q = 0$ limit Vergados and Kosmas gave the spin matrix element in the simple form $|\mathbf{J}|^2 = |f_A^0 \Omega_0(0) + f_A^1 \Omega_1(0)|^2$, and found that $\Omega_0(0) = -0.95659/\sqrt{3}$, and $\Omega_1(0) = 0.83296/\sqrt{3}$ [3, 13]. These values were recalculated in the form of spin variables $\langle \mathbf{S}_{p(n)} \rangle$ given in Table 13.

Ressel and Dean [6] have performed most accurate nuclear shell-model calculations of the neutralino–nucleus spin-dependent or axial cross section for several nuclei in the $A = 127$ region, which are important for dark matter search. Their set of structure functions $S(q)$ is valid for all relevant values of the momentum transfer. Conventional nuclear shell model of Wildenthal [36] quite accurately

represents spin-dependent neutralino–nucleus matrix elements when a reasonable nuclear Hamiltonian is used in a sufficiently large model space [6]. Until recently, both of these ingredients have been absent for nuclei in the $3s2d1g_{7/2}1h_{11/2}$ shell. Ressel and Dean considered two residual nuclear interactions based upon recently developed realistic nucleon–nucleon Bonn A [37] and Nijmegen II [38] potentials. These two nucleon–nucleon potentials were used in order to investigate the sensitivity of the results to the particular nuclear Hamiltonian.

The Bonn-A-based Hamiltonian has been derived for the model space consisting of the $1g_{7/2}$, $2d_{5/2}$, $3s_{1/2}$, $2d_{3/2}$, and $1h_{11/2}$ orbitals, allowing one to include all relevant correlations. In order to get good agreement with observables for nuclei with $A \approx 130$, the single-particle energies (SPEs) were adjusted. The SPEs were varied until reasonable agreement between calculation and experiment was found for the magnetic moment, the low-lying excited state energy spectrum, and the quadrupole moment of ^{127}I . Once the SPEs are specified, a reasonable Hamiltonian can be used for the nuclei under investigation.

To perform a full basis calculation of the ^{127}I ground state properties in the space consisting of the $1g_{7/2}$, $2d_{5/2}$, $3s_{1/2}$, $2d_{3/2}$, and $1h_{11/2}$ orbitals, one would need basis states consisting of roughly $1.3 \cdot 10^9$ Slater Determinants (SDs). Current calculations can diagonalize matrices with basis dimensions in the range $1\text{--}2 \cdot 10^7$ SDs. Therefore clearly severe truncations of the model space are needed [6]. Fortunately, given the size of the model spaces that can be treated, a truncation scheme that includes the majority of relevant configurations can be devised. Finally (after relevant truncations, see details in [6]) the m -scheme dimension of the ^{127}I model space is about 3 million SDs. The calculated observables agree well with experiment. These interactions do not seem to prefer excitation of more than one extra neutron pair to the $1h_{11/2}$. Most configurations have six neutrons in that orbital, while eight are allowed. Hence, this model space is more than adequate. It is this truncation scheme that was used for the two Xenon isotopes considered ($A = 129$ and 131).

In almost every instance, the results of [6] (Tables 8–10) show that the spin $\langle \mathbf{S}_i \rangle$ ($i = p, n$) carried by the unpaired nucleon is greater than that found in the other nuclear models (except for the ISPSM, where $\langle \mathbf{S}_i \rangle$ is maximal). Despite these larger values for $\langle \mathbf{S}_i \rangle$, these calculations have significant quenching of the magnetic moment and are in good agreement with experiment in all cases. The larger values of $\langle \mathbf{S}_i \rangle$ are due to the fact that more excitations of the even group of the nuclei were allowed [6]. The differences in the response due to the two forces is clearly visible in Tables 8–10. In all cases reasonable agreement between calculation and experiment for the magnetic moment (using free particle g factors) is achieved. It is obvious that the differences between the two calculations are nontrivial but they are quite a bit smaller than the differences coming from the use of alternate nuclear models. This shows that the interaction is not the primary uncertainty in calculations of the neutralino–nucleus spin cross sections [6].

The results obtained by Ressel and Dean give a factor of 20 increase in the iodine's sensitivity to spin-dependent scattering over that previously assumed. Due to the form factor suppression the sodium iodide detector's spin response is still dominated by ^{23}Na but not to the extent previously thought. For the remainder of the nuclei considered, Tables 8–10 also reveal increased scattering sensitivity, though much more modest [6].

Before finishing this section we, following Ressel and Dean [6], discuss the quenching problem and some related uncertainties. As is already noted above, the comparison of the computed magnetic moment and its experimental value has been used as the primary indicator of the calculation's reliability. This seems quite reasonable in the light of the similarities between the matrix elements in Eqs. (13) and (16). This prescription is not free of several potential problems [7,8]. Not only does μ depend upon the orbital angular momentum \mathbf{L}_i , but the spin angular momentum \mathbf{S}_i is subtly different. The neutralino–nucleus matrix element (13) results from the nonrelativistic reduction of the axial-vector current. Because of this, it is not strongly affected by meson exchange currents (MECs). The magnetic moment's spin operators, \mathbf{S}_i , are a result of the nonrelativistic reduction of the vector current. They can be strongly affected by MECs [7]. The effects of MECs upon μ are typically lumped together with several other effects to give effective g factors. Unfortunately, there is no hard and fast rule as to what effective g factors are the best. One usually chooses to remain with the free particle g factors. As an example of the potential uncertainties this ambiguity leads to, the calculated magnetic moments for these nuclei based on a reasonable set of effective g factors were also included in Tables 8–10. The «quenched» magnetic moments are the values in curled parentheses and the effective g factors used are: $g_n^s = -2.87$, $g_n^l = -0.1$, $g_p^s = 4.18$, and $g_p^l = 1.1$. The tables show that these g factors do little to improve the concordance between calculation and experiment [6]. A related concern involves the quenching of the (isovector) Gamow–Teller (GT) g factor, g_A [7,8]. The spin term of the GT operator also comes from the axial vector current and thus is closely related to the spin operators in Eq. (16). It is well established that most nuclear model calculations of GT strength require a reduction of the order of 20% in g_A [36]. Whether this quenching of g_A should also be applied to a_1 (the isovector neutralino–nucleon coupling constant) is unknown. Since there is no real guidance and magnetic moments obtained by Ressel and Dean agree well with experiment, it is very doubtful that any extra quenching of the spin matrix elements (or equivalently the coupling constants a_0 and a_1) is desirable for these nuclei in the calculation of neutralino–nucleus scattering rates. Nonetheless, it is useful to keep these potential uncertainties in mind when calculating scattering rates [6–8].

Tables 1–13 contain the fullest possible list of calculations of the nuclear zero-momentum spin properties considered in the literature for detection of spin-coupled WIMPs. The tables are obtained on the basis of relevant tables for $\langle \mathbf{S}_n^A \rangle$

and $\langle \mathbf{S}_p^A \rangle$ from [5–12, 14–16, 24, 29]. The OGM results of Ellis and Flores given in [28, 39, 40] in the form of $\lambda^2 J(J+1)$ were recalculated into $\langle \mathbf{S}_i \rangle$ and checked.

2. SUMMARY AND CONCLUSIONS

There is continuous theoretical and experimental interest in existence of dark-matter of the Universe. The best motivated nonbaryonic dark-matter candidates is the neutralino, the lightest supersymmetric particle. The motivation for supersymmetry arises naturally in modern theories of particle physics. In this work we discussed the spin-dependent interaction of neutralinos with odd mass nuclei. The nuclear structure plays an important role in determining the strength of the neutralino–nucleus cross section for this type of interaction. In the limit of zero momentum transfer the relevant physical quantities are the proton and neutron spin averages $\langle \mathbf{S}_{p(n)} \rangle$, which have to be evaluated within a proper nuclear model. These values determine the event rate expected in a direct dark-matter search experiment due to spin-dependent neutralino–nucleus interaction. In this work the calculation of spin-dependent matrix elements is reviewed. To our knowledge, a complete list of calculated spin matrix elements is presented for nuclei throughout the periodic table. We recall that only nuclei with an odd number of either protons or neutrons can have nonzero spin.

As is manifested in this review, practically every known nuclear model has been employed for evaluation of the spin matrix elements. The results show that spin matrix elements depend in general rather sensitively on the details of the nuclear structure. The phenomenological ISPSM (independent single-particle shell model) is fairly accurate only for light nuclei with near-closed shells, but in general it tends to overestimate the spin matrix elements and is inadequate. It was confirmed by the calculations within the OGM (odd group model) and the EOGM (extended OGM) utilizing magnetic moments and mirror β decays. However, detailed shell-model calculations found these phenomenological models to be inadequate. The odd-group model and shell-model treatments yielded good agreement for light nuclei, but as the atomic mass increases, there arouses a significant amount of configuration mixing not considered in the OGM. Unfortunately, the shell-model calculations are difficult for most medium-heavy and heavy isotopes because of the size of the matrices involved. The situation is improving due to advances in computer power and storage. There is a hope to construct model spaces that contain most of the nuclear configurations that are likely to dominate the spin response of nuclei. For open-shell medium-heavy and heavy nuclei the methods of choice for calculation of spin matrix elements are the Interacting Boson–Fermion Model, the Theory of Finite Fermion Systems and the Quasi Tamm–Dancoff Approximation. The most reliable values of $\langle \mathbf{S}_{p(n)} \rangle$ are considered to be those of the approach which reproduces well the

experimental value of the magnetic moment for a given isotope. The magnetic moment is extremely important, as it is the observable most closely related to the neutralino–nucleus scattering matrix element and has traditionally been used as a benchmark for the calculation accuracy.

There is an additional complication arising from the fact that the neutralino appears to be quite massive, perhaps heavier than 100 GeV. For such a heavy light supersymmetric particle and sufficiently heavy nuclei, the dependence of the nuclear matrix elements on the momentum transfer cannot be ignored. This affects the spin matrix elements. The calculations of the structure functions in the finite momentum approximation and the level of accuracy of these calculations are beyond the scope of this review.

This work was supported in part by the VEGA Grant Agency of the Slovak Republic under contract No. 1/0249/03 and by the Russian Foundation for Basic Research (grant No. 02-02-04009).

APPENDIX

A1. Elements of Nuclear Structure Calculations. The transverse electric $\mathcal{T}_L^{\text{el5}}(q)$ and longitudinal $\mathcal{L}_L^5(q)$ multipole projections of the axial vector current operator as well as the scalar function $\mathcal{C}_L(q)$ are given in [8, 12, 24]:

$$\begin{aligned}\mathcal{T}_L^{\text{el5}}(q) &= \frac{1}{\sqrt{2L+1}} \sum_i \frac{a_0 + a_1 \tau_3^i}{2} \left[-\sqrt{L} M_{L,L+1}(q\mathbf{r}_i) + \sqrt{L+1} M_{L,L-1}(q\mathbf{r}_i) \right], \\ \mathcal{L}_L^5(q) &= \frac{1}{\sqrt{2L+1}} \sum_i \left(\frac{a_0}{2} + \frac{a_1 m_\pi^2 \tau_3^i}{2(q^2 + m_\pi^2)} \right) \times \\ &\quad \times \left[\sqrt{L+1} M_{L,L+1}(q\mathbf{r}_i) + \sqrt{L} M_{L,L-1}(q\mathbf{r}_i) \right], \\ \mathcal{C}_L(q) &= \sum_{i, \text{ nucleons}} C_0^E j_L(qr_i) Y_L(\hat{r}_i), \quad \mathcal{C}_0(q) = \sum_i C_0^E j_0(qr_i) Y_0(\hat{r}_i),\end{aligned}\tag{22}$$

where $M_{L,L'}(q\mathbf{r}_i) = j_{L'}(qr_i) [Y_{L'}(\hat{r}_i) \sigma_i]^L$. In the limit of zero momentum transfer, $S_{\text{SD}}^A(q)$ reduces to

$$\begin{aligned}S_{\text{SD}}^A(0) &= \frac{1}{4\pi} \left| \langle N | \sum_i \frac{1}{2} (a_0 + a_1 \tau_3^i) \sigma_i | N \rangle \right|^2 = \\ &= \frac{1}{4\pi} |(a_0 + a_1) \langle N | \mathbf{S}_p | N \rangle + (a_0 - a_1) \langle N | \mathbf{S}_n | N \rangle|^2 = \tag{23} \\ &= \frac{1}{\pi} \frac{(2J+1)(J+1)}{J} |a_p \langle N | \mathbf{S}_p | N \rangle + a_n \langle N | \mathbf{S}_n | N \rangle|^2 = \\ &= \frac{2J+1}{\pi} J(J+1) \Lambda^2, \tag{24}\end{aligned}$$

with

$$\Lambda = \frac{\langle N | a_p \mathbf{S}_p + a_n \mathbf{S}_n | N \rangle}{J} = \frac{a_p \langle \mathbf{S}_p \rangle}{J} + \frac{a_n \langle \mathbf{S}_n \rangle}{J}.$$

In accordance with convention the Z components of the angular momentum and spin operators are evaluated in the maximal M_J state, e.g., $\langle \mathbf{S} \rangle \equiv \langle N | \mathbf{S} | N \rangle = \langle J, M_J = J | S_z | J, M_J = J \rangle$.

In the ISPSM only the last odd nucleon contributes to the spin and the angular momentum of the nucleus. In this limit

$$\langle \mathbf{S}_n^A \rangle = \frac{J_A(J_A + 1) - L_A(L_A + 1) + 3/4}{2J_A + 2}, \quad (25)$$

where J_A and L_A are the single-particle total and angular momenta. They are deduced from the measured nuclear angular momentum and the parity.

A2. Nucleon Spin Structure. To evaluate the spin content of the nucleon one needs the matrix element of the effective quark axial-vector current $J^\mu = \bar{q} \gamma^\mu \gamma_5 q$ in the nucleon [16]. These matrix elements

$$\langle (p, n) | \bar{q} \gamma_\mu \gamma_5 q | (p, n) \rangle = 2s_\mu^{(p,n)} \Delta q^{(p,n)} \quad (26)$$

are proportional to the spin of the neutron (proton or neutron), $s_\mu^{(p,n)}$. The quantities $\Delta q^{(p,n)}$ are usually extracted from the data obtained in polarized lepton–nucleon deep inelastic scattering. Uncertainties in the experimentally determined values for the quantities Δq can lead to significant variations in the WIMP–nucleon axial-vector coupling, and therefore to the predicted rates for detection of WIMPs which have primarily spin couplings to nuclei [16]. With definition (26) the effective spin-dependent interaction of neutralinos with the nucleon has the form

$$\mathcal{L}_{\text{spin}} = 2\bar{\chi} \gamma^\mu \gamma_5 \chi \bar{n} s_\mu n \sum_{q=u,d,s} \mathcal{A}_q \Delta q^{(n)}. \quad (27)$$

Recent global QCD analysis for the g_1 -structure functions [41], including $\mathcal{O}(\alpha_s^3)$ corrections, corresponds to the following values of spin nucleon parameters [42]:

$$\begin{aligned} \Delta_u^{(p)} &= \Delta_d^{(n)} = 0.78 \pm 0.02, \\ \Delta_d^{(p)} &= \Delta_u^{(n)} = -0.48 \pm 0.02, \\ \Delta_s^{(p)} &= \Delta_s^{(n)} = -0.15 \pm 0.02. \end{aligned}$$

A3. Effective Neutralino–Quark Lagrangian. The axial-vector and scalar interaction of a neutralino with a quark q is given by

$$\mathcal{L}_{\text{eff}} = \mathcal{A}_q \bar{\chi} \gamma_\mu \gamma_5 \chi \bar{q} \gamma^\mu \gamma_5 q + \mathcal{C}_q \bar{\chi} \chi \bar{q} q + \mathcal{O}(1/m_{\tilde{q}}^4).$$

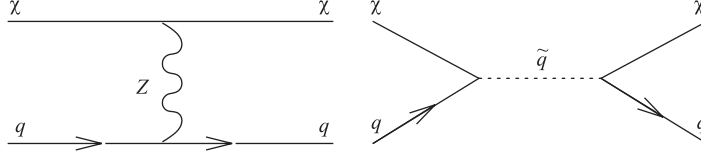


Fig. 1. Spin-dependent elastic scattering of neutralinos from quarks

The terms with vector and pseudoscalar quark currents are omitted being negligible in the case of nonrelativistic DM neutralinos with typical velocities $v_\chi \approx 10^{-3}c$. The Feynman diagrams which give rise to the effective neutralino–quark axial-vector couplings

$$\begin{aligned} \mathcal{A}_q = & -\frac{g^2}{4M_W^2} \left[\frac{\mathcal{N}_{14}^2 - \mathcal{N}_{13}^2}{2} T_3 - \right. \\ & - \frac{M_W^2}{m_{\tilde{q}_1}^2 - (m_\chi + m_q)^2} (\cos^2 \theta_q \phi_{qL}^2 + \sin^2 \theta_q \phi_{qR}^2) - \\ & - \frac{M_W^2}{m_{\tilde{q}_2}^2 - (m_\chi + m_q)^2} (\sin^2 \theta_q \phi_{qL}^2 + \cos^2 \theta_q \phi_{qR}^2) - \\ & - \frac{m_q^2}{4} P_q^2 \left(\frac{1}{m_{\tilde{q}_1}^2 - (m_\chi + m_q)^2} + \frac{1}{m_{\tilde{q}_2}^2 - (m_\chi + m_q)^2} \right) - \\ & - \frac{m_q}{2} M_W P_q \sin 2\theta_q T_3 (\mathcal{N}_{12} - \tan \theta_W \mathcal{N}_{11}) \times \\ & \left. \times \left(\frac{1}{m_{\tilde{q}_1}^2 - (m_\chi + m_q)^2} - \frac{1}{m_{\tilde{q}_2}^2 - (m_\chi + m_q)^2} \right) \right] \end{aligned}$$

are shown in Fig. 1. The first term in \mathcal{A}_q comes from Z^0 exchange, and the other terms come from squark exchanges. The Feynman diagrams which give rise to the effective neutralino–quark scalar couplings

$$\begin{aligned} \mathcal{C}_q = & -\frac{m_q}{M_W} \frac{g^2}{4} \left[\frac{F_h}{m_h^2} h_q + \frac{F_H}{m_H^2} H_q + \left(\frac{m_q}{4M_W} P_q^2 - \frac{M_W}{m_q} \phi_{qL} \phi_{qR} \right) \times \right. \\ & \times \left(\frac{\sin 2\theta_q}{m_{\tilde{q}_1}^2 - (m_\chi + m_q)^2} - \frac{\sin 2\theta_q}{m_{\tilde{q}_2}^2 - (m_\chi + m_q)^2} \right) + \\ & \left. + P_q \left(\frac{\cos^2 \theta_q \phi_{qL} - \sin^2 \theta_q \phi_{qR}}{m_{\tilde{q}_1}^2 - (m_\chi + m_q)^2} - \frac{\cos^2 \theta_q \phi_{qR} - \sin^2 \theta_q \phi_{qL}}{m_{\tilde{q}_2}^2 - (m_\chi + m_q)^2} \right) \right], \end{aligned}$$

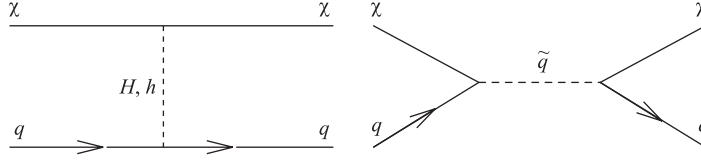


Fig. 2. Spin-independent or scalar (tree level) elastic scattering of neutralinos from quarks

where

$$\begin{aligned}
 F_h &= (\mathcal{N}_{12} - \mathcal{N}_{11} \tan \theta_W)(\mathcal{N}_{14} \cos \alpha_H + \mathcal{N}_{13} \sin \alpha_H), \\
 F_H &= (\mathcal{N}_{12} - \mathcal{N}_{11} \tan \theta_W)(\mathcal{N}_{14} \sin \alpha_H - \mathcal{N}_{13} \cos \alpha_H), \\
 h_q &= \left(\frac{1}{2} + T_3\right) \frac{\cos \alpha_H}{\sin \beta} - \left(\frac{1}{2} - T_3\right) \frac{\sin \alpha_H}{\cos \beta}, \\
 H_q &= \left(\frac{1}{2} + T_3\right) \frac{\sin \alpha_H}{\sin \beta} + \left(\frac{1}{2} - T_3\right) \frac{\cos \alpha_H}{\cos \beta}, \\
 \phi_{qL} &= \mathcal{N}_{12} T_3 + \mathcal{N}_{11}(Q - T_3) \tan \theta_W, \quad \phi_{qR} = \tan \theta_W Q \mathcal{N}_{11}, \\
 P_q &= \left(\frac{1}{2} + T_3\right) \frac{\mathcal{N}_{14}}{\sin \beta} + \left(\frac{1}{2} - T_3\right) \frac{\mathcal{N}_{13}}{\cos \beta},
 \end{aligned}$$

are shown in Fig. 2. The importance of these scalar spin-independent contribution was found by K. Griest in [43].

A4. SUSY Particle Spectrum. For completeness, we collect here formulas for masses of the SUSY particles in the MSSM. There are four Higgs bosons — neutral CP -odd (A), CP -even (H, h), charged (H^\pm). The CP -even Higgs boson mass matrix has the form:

$$\begin{pmatrix} H_{11} & H_{12} \\ H_{12} & H_{22} \end{pmatrix} = \frac{1}{2} \begin{pmatrix} \tan \beta & -1 \\ -1 & \cot \beta \end{pmatrix} M_A^2 \sin 2\beta + \\
 + \frac{1}{2} \begin{pmatrix} \cot \beta & -1 \\ -1 & \tan \beta \end{pmatrix} m_Z^2 \sin 2\beta + \omega \begin{pmatrix} \Delta_{11} & \Delta_{12} \\ \Delta_{12} & \Delta_{22} \end{pmatrix},$$

$$H_{11} = \frac{\sin 2\beta}{2} \left(\frac{m_Z^2}{\tan \beta} + M_A^2 \tan \beta \right) + \omega \Delta_{11},$$

$$H_{22} = \frac{\sin 2\beta}{2} \left(m_Z^2 \tan \beta + \frac{M_A^2}{\tan \beta} \right) + \omega \Delta_{22},$$

$$H_{12} = H_{21}^2 = -\frac{\sin 2\beta}{2} (m_Z^2 + M_A^2) + \omega \Delta_{12}.$$

For example, Δ_{11} which includes loop corrections is

$$\begin{aligned} \Delta_{11} = & \frac{m_b^4}{c_\beta^2} \left(\ln \frac{m_{b_1}^2 m_{b_2}^2}{m_b^4} + \frac{2A_b(A_b - \mu \tan \beta)}{m_{b_1}^2 - m_{b_2}^2} \ln \frac{m_{b_1}^2}{m_{b_2}^2} \right) + \\ & + \frac{m_b^4}{c_\beta^2} \left(\frac{A_b(A_b - \mu \tan \beta)}{m_{b_1}^2 - m_{b_2}^2} \right)^2 g(m_{b_1}^2, m_{b_2}^2) + \\ & + \frac{m_t^4}{s_\beta^2} \left(\frac{\mu \left(A_t - \frac{\mu}{\tan \beta} \right)}{m_{t_1}^2 - m_{t_2}^2} \right)^2 g(m_{t_1}^2, m_{t_2}^2), \end{aligned}$$

where $\omega = \frac{3g_2^2}{16\pi^2 m_W^2}$, $c_\beta^2 = \cos^2 \beta$, $s_\beta^2 = \sin^2 \beta$, $g(m_1^2, m_2^2) = 2 - \frac{m_1^2 + m_2^2}{m_1^2 - m_2^2} \ln \frac{m_1^2}{m_2^2}$.

The diagonalization of the above matrix gives the Higgs boson masses:

$$\begin{aligned} m_{H,h}^2 &= \frac{1}{2} \left\{ H_{11} + H_{22} \pm \sqrt{(H_{11} + H_{22})^2 - 4(H_{11}H_{22} - H_{12}^2)} \right\}, \\ m_{H^\pm}^2 &= m_W^2 + M_A^2 + \omega \Delta_{\text{ch}}. \end{aligned}$$

Here m_{H^\pm} is the charged Higgs boson mass in the one-loop approximation. The mixing angle α_H is obtained from

$$\sin 2\alpha_H = \frac{2H_{12}^2}{m_{H_1^0}^2 - m_{H_2^0}^2}, \quad \cos 2\alpha_H = \frac{H_{11}^2 - H_{22}^2}{m_{H_1^0}^2 - m_{H_2^0}^2}.$$

The neutralino mass matrix in the basis $(\tilde{B}, \tilde{W}^3, \tilde{H}_1^0, \tilde{H}_2^0)$ has the form:

$$\mathcal{M}_\chi = \begin{pmatrix} M_1 & 0 & -M_Z \cos \beta \sin \theta_W & M_Z \sin \beta \sin \theta_W \\ 0 & M_2 & M_Z \cos \beta \cos \theta_W & -M_Z \sin \beta \cos \theta_W \\ -M_Z \cos \beta \sin \theta_W & M_Z \cos \beta \cos \theta_W & 0 & -\mu \\ M_Z \sin \beta \sin \theta_W & -M_Z \sin \beta \cos \theta_W & -\mu & 0 \end{pmatrix}.$$

The diagonalization gives mass eigenstates (4 neutralinos):

$$\chi_i(m_{\chi_i}) = \mathcal{N}_{i1} \tilde{B} + \mathcal{N}_{i2} \tilde{W}^3 + \mathcal{N}_{i3} \tilde{H}_1^0 + \mathcal{N}_{i4} \tilde{H}_2^0.$$

The lightest (LSP) $\chi = \chi_1$ is the best DM candidate. The chargino mass term is

$$\left(\tilde{W}^-, \tilde{H}_1^- \right) \begin{pmatrix} M_2 & \sqrt{2} M_W \sin \beta \\ \sqrt{2} M_W \cos \beta & \mu \end{pmatrix} \begin{pmatrix} \tilde{W}^+ \\ \tilde{H}_2^+ \end{pmatrix} + \text{h.c.}$$

The diagonalization $U^* \mathcal{M}_{\tilde{\chi}^\pm} V^\dagger = \text{diag}(M_{\tilde{\chi}_1^\pm}, M_{\tilde{\chi}_2^\pm})$ gives charged mass eigenstates

$$\tilde{\chi}^- = U_{i1} \tilde{W}^- + U_{i2} \tilde{H}^-, \quad \tilde{\chi}^+ = V_{i1} \tilde{W}^+ + V_{i2} \tilde{H}^+$$

with masses

$$M_{\tilde{\chi}_{1,2}^\pm}^2 = \frac{1}{2} \left[M_2^2 + \mu^2 + 2M_W^2 \mp \sqrt{(M_2^2 - \mu^2)^2 + 4M_W^4 \cos^2 2\beta + 4M_W^2 (M_2^2 + \mu^2 + 2M_2 \mu \sin 2\beta)} \right].$$

The sfermion mass matrices \mathcal{M}_t^2 , \mathcal{M}_b^2 , and \mathcal{M}_τ^2 have the form:

$$\mathcal{M}_t^2 = \begin{bmatrix} m_Q^2 + m_t^2 + \frac{1}{6}(4M_W^2 - M_Z^2) \cos 2\beta & m_t(A_t - \mu \cot \beta) \\ m_t(A_t - \mu \cot \beta) & m_U^2 + m_t^2 - \frac{2}{3}(M_W^2 - M_Z^2) \cos 2\beta \end{bmatrix},$$

$$\mathcal{M}_b^2 = \begin{bmatrix} m_Q^2 + m_b^2 - \frac{1}{6}(2M_W^2 + M_Z^2) \cos 2\beta & m_b(A_b - \mu \tan \beta) \\ m_b(A_b - \mu \tan \beta) & m_D^2 + m_b^2 + \frac{1}{3}(M_W^2 - M_Z^2) \cos 2\beta \end{bmatrix},$$

$$\mathcal{M}_\tau^2 = \begin{bmatrix} m_L^2 + m_\tau^2 - \frac{1}{2}(2M_W^2 - M_Z^2) \cos 2\beta & m_\tau(A_\tau - \mu \tan \beta) \\ m_\tau(A_\tau - \mu \tan \beta) & m_E^2 + m_\tau^2 + (M_W^2 - M_Z^2) \cos 2\beta \end{bmatrix}.$$

It is worth noting that these masses as well as the above-mentioned couplings of neutralino–quark interactions \mathcal{A}_q and \mathcal{C}_q are functions of the common set of SUSY parameters like, for example, $\tan \beta$, M_A , μ , A_q , etc. The set of parameters allows one to describe observables at the highest and lowest energies coherently and simultaneously.

REFERENCES

1. *Bernabei R. et al.* Dark-matter search // Riv. Nuovo Cim. 2003. V. 26. P. 1–73; astro-ph/0307403.
2. *Bednyakov V. A., Klapdor-Kleingrothaus H. V.* Update of the direct detection of dark matter and the role of the nuclear spin // Phys. Rev. D. 2001. V. 63. P. 095005; hep-ph/0011233;
Bednyakov V. A., Klapdor-Kleingrothaus H. V. On dark matter search after DAMA with Ge-73. hep-ph/0404102.
3. *Vergados J. D.* Searching for cold dark matter // J. Phys. G. 1996. V. 22. P. 253–272; hep-ph/9504320.
4. *Vergados J. D.* SUSY dark matter in the universe: Theoretical direct detection rates // Phys. At. Nucl. 2003. V. 66. P. 481–489; hep-ph/0201014.
5. *Divari P. C. et al.* Shell model calculations for light supersymmetric particle scattering off light nuclei // Phys. Rev. C. 2000. V. 61. P. 054612.
6. *Ressell M. T., Dean D. J.* Spin-dependent neutralino nucleus scattering for A approx. 127 nuclei // Phys. Rev. C. 1997. V. 56. P. 535–546; hep-ph/9702290.

7. *Engel J. et al.* Response of mica to weakly interacting massive particles // *Phys. Rev. C.* 1995. V. 52. P. 2216–2221; hep-ph/9504322.
8. *Ressell M. T. et al.* Nuclear shell model calculations of neutralino — nucleus cross-sections for Si-29 and Ge-73 // *Phys. Rev. D.* 1993. V. 48. P. 5519–5535.
9. *Dimitrov V., Engel J., Pittel S.* Scattering of weakly interacting massive particles from Ge-73 // *Phys. Rev. D.* 1995. V. 51. P. 291–295; hep-ph/9408246.
10. *Engel J. et al.* Scattering of neutralinos from niobium // *Phys. Lett. B.* 1992. V. 275. P. 119–123.
11. *Nikolaev M. A., Klapdor-Kleingrothaus H. V.* Effects of nuclear structure in the spin-dependent scattering of weakly interacting massive particles // *Z. Phys. A.* 1993. V. 345. P. 183–186.
12. *Engel J.* Nuclear form factors for the scattering of weakly interacting massive particles // *Phys. Lett. B.* 1991. V. 264. P. 114–119.
13. *Kosmas T. S., Vergados J. D.* Cold dark matter in SUSY theories. The role of nuclear form factors and the folding with the LSP velocity // *Phys. Rev. D.* 1997. V. 55. P. 1752–1764; hep-ph/9701205.
14. *Pacheco A. F., Strottman D.* Nuclear structure corrections to estimates of the spin-dependent WIMP nucleus cross-section // *Phys. Rev. D.* 1989. V. 40. P. 2131–2133.
15. *Iachello F., Krauss L. M., Maino G.* Spin-dependent scattering of weakly interacting massive particles in heavy nuclei // *Phys. Lett. B.* 1991. V. 254. P. 220–224.
16. *Jungman G., Kamionkowski M., Griest K.* Supersymmetric dark matter // *Phys. Rep.* 1996. V. 267. P. 195–373; hep-ph/9506380.
17. *Lewin J. D., Smith P. F.* Review of mathematics, numerical factors, and corrections for dark-matter experiments based on elastic nuclear recoil // *Astropart. Phys.* 1996. V. 6. P. 87–112.
18. *Smith P. F., Lewin J. D.* Dark matter detection // *Phys. Rep.* 1990. V. 187. P. 203.
19. *Bednyakov V. A., Klapdor-Kleingrothaus H. V.* Possibilities of directly detecting dark-matter particles in the next-to-minimal supersymmetric standard model // *Phys. At. Nucl.* 1999. V. 62. P. 966–974.
20. *Bednyakov V. A., Kovalenko S. G., Klapdor-Kleingrothaus H. V.* Prospects in searches for cosmic dark matter in underground experiments // *Phys. At. Nucl.* 1996. V. 59. P. 1718–1727.
21. *Bednyakov V. A., Klapdor-Kleingrothaus H. V., Kovalenko S. G.* Superlight neutralino as a dark-matter particle candidate // *Phys. Rev. D.* 1997. V. 55. P. 503–514; hep-ph/9608241.
22. *Bednyakov V. A. et al.* Is SUSY accessible by direct dark-matter detection? // *Z. Phys. A.* 1997. V. 357. P. 339–347; hep-ph/9606261.
23. *Bednyakov V. A., Klapdor-Kleingrothaus H. V., Kovalenko S. G.* On SUSY dark-matter detection with spinless nuclei // *Phys. Rev. D.* 1994. V. 50. P. 7128–7143; hep-ph/9401262.
24. *Engel J., Pittel S., Vogel P.* Nuclear physics of dark-matter detection // *Intern. J. Mod. Phys. E.* 1992. V. 1. P. 1–37.
25. *Griest K.* Cross sections, relic abundance, and detection rates for neutralino dark matter // *Phys. Rev. D.* 1988. V. 38. P. 2357.
26. *Goodman M. W., Witten E.* Detectability of certain dark-matter candidates // *Phys. Rev. D.* 1985. V. 31. P. 3059.
27. *Drukier A. K., Freese K., Spergel D. N.* Detecting cold dark-matter candidates // *Phys. Rev. D.* 1986. V. 33. P. 3495–3508.
28. *Ellis J. R., Flores R. A.* Realistic predictions for the detection of supersymmetric dark matter // *Nucl. Phys. B.* 1988. V. 307. P. 883.

29. *Engel J., Vogel P.* Spin-dependent cross-sections of weakly interacting massive particles on nuclei // *Phys. Rev. D.* 1989. V. 40. P. 3132–3135.
30. *Nikolaev M. A., Klapdor-Kleingrothaus H. V.* Quenching of the spin-dependent scattering of weakly interacting massive particles on heavy nuclei // *Z. Phys. A.* 1993. V. 345. P. 373–376.
31. *Cohen S., Kurath D.* Effective interactions for the $1p$ shell // *Nucl. Phys.* 1965. V. 73. P. 1–24.
32. *Resler D., Grimes S.* CRUNCHER code // *Comp. Phys.* 1988. V. 2, No. 3. P. 65–66.
33. *Towner I.* Quenching of spin matrix elements in nuclei // *Phys. Rep.* 1987. V. 155, No. 5. P. 263–377.
34. *Petrovich F. et al.* // *Phys. Rev. Lett.* 1969. V. 38. P. 895.
35. *Dimitrov V.* Hybrid symmetry-conserving variational procedure for nuclear structure calculations // *Phys. Rev. C.* 1994. V. 50. P. 2893–2899.
36. *Brown B., Wildenthal B.* // *Ann. Rev. Nucl. Part. Sci.* 1988. V. 38. P. 29.
37. *Hjorth-Jensen M., Kuo T. T. S., Osnes E.* Realistic effective interactions for nuclear systems // *Phys. Rep.* 1995. V. 261. P. 125–270.
38. *Stoks V. G. J. et al.* Construction of high quality NN potential models // *Phys. Rev. C.* 1994. V. 49. P. 2950–2962; nucl-th/9406039.
39. *Ellis J. R., Flores R. A.* Elastic supersymmetric relic — nucleus scattering revisited // *Phys. Lett. B.* 1991. V. 263. P. 259–266.
40. *Ellis J. R., Flores R. A.* Implications of LEP on laboratory searches for dark-matter neutralinos // *Nucl. Phys. B.* 1993. V. 400. P. 25–36.
41. *Mallot G. K.* The spin structure of the nucleon // *Intern. J. Mod. Phys. A.* 2000. V. 15S1. P. 521–537; hep-ex/9912040.
42. *Ellis J. R., Ferstl A., Olive K. A.* Re-evaluation of the elastic scattering of supersymmetric dark matter // *Phys. Lett. B.* 2000. V. 481. P. 304–314; hep-ph/0001005.
43. *Griest K.* Calculations of rates for direct detection of neutralino dark matter // *Phys. Rev. Lett.* 1988. V. 61. P. 666.